STATE HIGHWAY ADMINISTRATION

RESEARCH REPORT

INTEGRATION OF OFF-RAMP AND ARTERIAL SIGNAL CONTROLS TO MINIMIZE THE RECURRENT CONGESTION ON THE I-495 CAPTIAL BELTWAY

Dr. Gang-Len Chang
Zhuan LI

Department of Civil and Environmental Engineering
University of Maryland
College Park, MD 20742

Project number MD-08-SP808B4D

June 2010

Technical Report Documentation Page

1. Report No. **MD-08-SP808B4D**	2. Government Accession No.	3. Recipient's Catalog No.
4. Title and Subtitle Integration of Off-ramp and Arterial Signal Controls to Minimize the Recurrent Congestion on the I-495 Capital Beltway		5. Report Date June 7, 2010
		6. Performing Organization Code
7. Author/s Dr. Gang-Len Chang Zichuan Li		8. Performing Organization Report No.
9. Performing Organization Name and Address Department of Civil and Environmental Engineering, University of Maryland, College Park, MD 20742		10. Work Unit No. (TRAIS)
		11. Contract or Grant No. **SP808B4D**
12. Sponsoring Organization Name and Address Maryland State Highway Administration Office of Policy & Research 707 North Calvert Street Baltimore MD 21202		13. Type of Report and Period Covered Draft Report
		14. Sponsoring Agency Code (7120) STMD - MDOT/SHA

16. Abstract

This study developed an integrated control model to contend with the impact of off-ramp queue spillback on both the freeway and arterials within the interchange control boundaries. The proposed model consists of two levels that compute the optimal coordinated signal strategies for intersections and off-ramps. Whereas the first level primarily handles oversaturated flows and blockage between lanes at congested intersections, the second level deals with the freeway mainline delays caused by the excessive off-ramp queue spillback; these components work together to produce the optimal system-wide signal and ramp control plans. In addition to developing control modules for oversaturated arterials and excessive off-ramp queues, the study also conducted some experimental analysis using field data from the interchange at I-495 and Georgia Avenue. The experimental results indicate that, by accounting for how off-ramp queues impact delays of both freeway and arterial traffic, the interchange system optimal control can yield the best use of a roadway's overall capacity and prevent the formation of freeway queues in the interchange area caused by the overflow of off-ramp traffic.

17. Key Words off-ramp control, arterial optimization, signal	18. Distribution Statement: No restrictions This document is available from the Research Division upon request.		
19. Security Classification (of this report) None	20. Security Classification (of this page) None	21. No. Of Pages	22. Price

Form DOT F 1700.7 (8-72) Reproduction of form and completed page is authorized.

CONTENTS

CHAPTER 1: INTRODUCTION

1.1 Research Background

Effectively contending with the growing congestion on the Capital Beltway has long been the top priority and the most challenging task of transportation professionals in this region. Although a variety of factors has contributed to its deteriorating traffic conditions, the insufficient capacity of the mainline to accommodate the ever-increasing demand from the Washington Metropolitan Area is certainly the top issue to address. Our extensive field observations of the congestion patterns on the Capital Beltway over recent years have revealed that many existing bottlenecks during peak hours are due to the spillback of the traffic queue from an off-ramp that often takes away the capacity of one to two mainline travel lanes when it exceeds the length of an auxiliary lane. Examples of bottlenecks caused by such off-ramp spillback vehicles can be found at the Connecticut Avenue and Georgia Avenue interchanges during peak hours. Thus, while policy makers explore demand-side methods, such as congestion pricing and HOT lanes, it is essential that the potentially cost-effective and near-term deployable strategy of integrated off-ramp control be investigated.

Thus, we propose the design of a control system for the integrated operation of off-ramps and their local arterial signals with two layers of operational objectives. The first layer involves implementing a monitoring mechanism that can prevent off-ramp vehicles from spilling back into the mainline, thereby reducing its capacity. The second layer will apply optimal control theory to maximize the throughput of the target roadway segment, including both the off-ramp and its upstream and downstream intersections. Depending on traffic conditions and the available capacity of the target local arterial, one shall investigate the impacts of assigning different priorities to the off-ramp vehicles on the arterial traffic progression and flow speed, if the off-ramp queue has been controlled within the auxiliary lane.

It should be mentioned that traffic bottlenecks caused by off-ramp spillback queues are quite common congestion patterns on many metropolitan beltways. Neither research institutions nor operational agencies have developed effective strategies to contend with their impacts on mainline capacity. Our pioneering efforts on this issue will

be able to make significant contributions to both our state and the nationwide highway networks.

1.2 Research Objectives and Project Scope

To meet its primary objective, this study has developed an integrated off-ramp and arterial signal control system for urban interchanges that can adjust the signal plan to minimize the queue spillback from off-ramps to the freeway mainline while maximizing throughput on their neighboring arterials. To do so, the proposed system has contained two principal components: (1) a set of real-time control algorithms to optimize the signal timing plans at those intersections within the impact area of the off-ramp flows; and (2) an interchange simulator to provide real-time feedback evaluation of traffic conditions on both the freeway and its neighboring arterial segments within the control area.

Unlike most existing studies on interchange traffic control, this research focuses on contending with the scenario in which traffic volumes on both the freeway and its local arterial are high enough to cause intersection overflow and off-ramp spillback to the freeway mainline segment. Hence, the development of control algorithms to optimize the overall operational efficiency for such congested interchanges needs to consider the tradeoff between freeway and arterial traffic delays, while also accounting for potential lane blockages at local intersections due to oversaturated traffic conditions during different control periods.

Note that, since most target interchanges on the I-495 Capital Beltway consist of several on- and off-ramps and intersections, it is essential to ensure that implementing the optimal systemwide control will not cause any undesirable local consequences, such as increasing the left-turn queue length at a particular intersection. Thus, the scope of this study also includes a comprehensive sensitivity analysis of all possible traffic scenarios, based on field data from the interchange of I-495 and George Avenue, and the selection of operational constraints for each control point at the overall system optimization process.

1.3 Report Organization

To take advantage of existing studies on this vital issue, we have conducted an extensive literature review of the available interchange and corridor control models and

reported our findings in Chapter 2. Since signal design and ramp operational strategies are the two principal components of our proposed integrated interchange control system, that chapter also summarizes some state-of-the-art developments associated with both vital research issues.

Chapter 3 presents the overall framework for the proposed integrated control system, including the interrelationships between all principal components, the operational flowchart, and potential extensions to a corridor-level control.

Chapter 4 details the proposed arterial control component, which functions to generate the set of time-varying optimal timing plans for each signal within the control boundaries during the congested peak hours. It includes an analysis of the complex interrelations between the signal phasing plan and the distribution of traffic volumes and formulations for mutual traffic blockages between lanes under spillback conditions. This chapter also focuses on the modeling methodology used to integrate traffic conditions at all intersections and ramps in an operational optimal control model.

Chapter 5 illustrates the advanced interchange control system, which includes the proposed arterial component, but further considers the potential impacts of off-ramp queue spillback on freeway through traffic. This chapter focuses on formulations of the freeway mainline traffic delay and its interdependent relationships with the traffic volume on the local arterials. The chapter also looks at how to select the proper control objective for the target interchange system under various congestion levels and how best to use the resulting measures of effectiveness (MOE).

Chapter 6 reports the results of evaluating the proposed integrated control system with field data from the interchange between I-495 (the Capital Beltway) and Georgia Avenue. It includes the design of many traffic scenarios based on the collected field data and their range of variation; it also uses the simulator to evaluate the performance of the optimal control strategies generated from the proposed integrated control system. This chapter also analyzes the essential subject of how best to use the computed optimal results for systemwide control operations without yielding unacceptable levels of service at any local control junctions.

Chapter 7 summarizes the primary research findings from this study, including valuable lessons obtained from developing the model and evaluating the system with

field data. Concluding comments, along with potential operation issues that may incur in future field system operations, are also the main focus of this chapter.

CHAPTER 2: LITERATURE REVIEW

2.1   Introduction

To take best advantage of existing studies on freeway control and interchange traffic management, we extensively reviewed the related literature covering integrated interchange control, ramp metering, and signal optimization. Critical issues and technical constraints identified from the literature actually served as the basis for finalizing the research objectives and scope of this study.

This chapter is organized as follows: Section 2.2 presents state-of-the-art models for interchange control, including strategies for both freeway ramps and their neighboring arterial signals. Section 2.3 reviews integrated models for corridor control, as their core modeling methods are all applicable for use in contending with queue formation and dissipation around a congested interchange. Section 2.4 summarizes existing studies for freeway access control, including both on- and off-ramps, which are often the locations that become the bottlenecks. Section 2.5 and section 2.6 highlight the strengths and deficiencies of the literature on arterial signal optimization, especially regarding effectively tackling traffic flows at oversaturated intersection.

2.2   Integrated Interchange Control Strategies

Integrated interchange control refers to controlling the interchange signals and on-ramp meters in an integrated manner. Many researchers over the past several decades have worked on this problem, and some have converted their research results into commercial products (Munjal, 1971; Messer and Berry, 1975; Messer, Fambro et al., 1977; Radwan and Hatton, 1990; Dorothy, Maleck et al., 1998; Chlewicki, 2003). For instance, Venglar et al. (1998) developed PASSER III, a computer program designed to analyze the operation of an isolated interchange. Engelbrecht and Barnes (2003) investigated eight possible controller features to improve the operations of diamond interchanges under moderate traffic conditions. However, most early studies on this subject focused only on under-saturated conditions, not congested scenarios where queue spillback may take place at either an off- or on-ramp, and the overflow blockage between lanes may occur at neighboring intersections.

More recently, Kovvali et al. (2002) began to address the issue of optimizing the control for congested interchanges and proposed an extension to PASSER III with a GA (genetic algorithm)-based model which can optimize the diamond interchange signals for both undersaturated and oversaturated traffic conditions with link queue spillback. The core logic of their proposed method involved employing the delay equations in the Highway Capacity Manual (HCM) and the platoon dispersion model in TRANSYT-7F to capture the dynamic interrelationships between the spatial evolution of traffic flows and the resulting delay under different signal plans.

Building on the work by Kovvali, some researchers (Tian and Messer et al., 2004) tackled the on-ramp spillback problem using an integrated model that concurrently optimized on-ramp metering and interchange signal control parameters. Further, Lee and Messer et al. (2006) conducted field investigation of the performance of actuated controls used at diamond interchanges under congested conditions.

Along the same lines, Fang and Elefteriadou (2006) proposed a different solution algorithm with a forward dynamic programming method that was adaptive in nature and thus responsive to fluctuating traffic demand evolving from moderate to congested conditions. Li, Chang et al. (2009) proposed a model to prevent off-ramp queues from spilling back to the freeway mainline segment by controlling the adjacent arterial signals. Zhang, et al. (2009) attempted to use a local synchronization control scheme for the same type of congested interchange. Their core control logic was to manage the queues at critical locations by coordinating traffic signals at neighboring intersections and freeway on-ramp meters. The model formulations for network traffic dynamics are represented with the traditional cell transmission concept.

In summary, although recent studies on the subject of interchange control have started to address complex interactions between congested traffic flows and the resulting on-ramp queues, many vital issues arising during oversaturated conditions remain to be tackled, such as overflow blockage between through and turning vehicles on local arterials and the spillback of off-ramp queues impeding freeway mainline traffic.

2.3   Integrated Corridor Control Model

Integrated corridor control refers to the concurrent optimization of freeway ramp flows and signal timing plans on adjacent arterials so as to maximize the throughput of the entire system. Since an interchange is a subsystem of a traffic corridor, many modeling concepts or creative algorithms proposed in the literature for these two traffic control types share the same potential for applications. Thus, this section also briefly reviews related modeling strategies in the literature for integrated corridor control.

Most existing studies of corridor control fall into one of the two following categories: (1) heuristic methods, along with simulation analysis for feedback adjustment control strategies; and (2) mathematical formulations with traffic flow and control theories. Some early studies that are examples of using heuristic methods include the control process proposed by Reiss (1981) and Van Aerde and Yagar (1988), both of which rely on simulation programs to evaluate the effectiveness of the proposed methods and to make necessary adjustments. Another study of the same type, conducted by Pooran and Sumner (1996), identified four types of coordination strategies and sixteen types of control tactics for managing corridor traffic.

In the second category, Cremer and Schoof (1989) were the first researchers to formulate an integrated corridor control model that included off-ramp traffic diversion, on-ramp metering, mainline speed limit control, and signal timing plans on the surface streets. They modeled freeway traffic dynamics with the classical continuous flow model and the arterial flow evolution with the platoon dispersion model from TRANSYT. The proposed solution algorithm is a mixed-integer nonlinear optimal control model along with a heuristic decomposition approach. Van Den Berg et al. (2004) proposed a model predictive control (MPC) approach for mixed urban and freeway traffic in urban corridors, based on enhanced macroscopic traffic flow formulations. Their study represents freeway dynamics with a continuous flow model, and reflects the horizontal and destination-dependent queues on urban arterials with a study by Kashani and Saridis (1983). Their model has the overall control objective of minimizing the total system travel time.

Grounded on a similar core theory, but with different formulations for traffic flow interactions between successive control segments, Chang et al. (1993) presented a

dynamic system-optimal control model for a commuting corridor consisting of a freeway and a parallel arterial. Their proposed formulations integrated ramp metering control with arterial signal optimization under the common functional objective of minimizing the total corridor travel time, and solved all control parameters concurrently with a linear approximation algorithm.

Focusing mainly on noncurrent congestion in commuting corridors, Wu and Chang (1999) later formulated a linear programming model with a heuristic algorithm to solve for the optimal ramp metering rate, the off-ramp diversion percentage, and arterial signal timing plans. Their proposed methodology employs classical traffic flow conservation relationships to capture the temporal and spatial evolution of vehicle flow on each segment of the freeway and arterial, including the flow transition between roadway segments and the flow discharge at intersections. To improve the computing speed for a large corridor network, this study further proposed a two-regime approximation for the nonlinear speed-density relationship that allows the application of a specially designed successive linear programming algorithm to solve the system-wide optimal state.

Along the same line of research, Papageorgiou (1995) developed a similar model to address corridor traffic management but used classical optimal control theory to model the traffic flow dynamics and the store-and-forward recursive relationship to reflect the feedback interrelations between the observed traffic conditions and the responsive adjustment of the control strategies. Tian and Balke (2002) analyzed the effectiveness of the integrated operation of surface street and freeway systems with VISSIM, a micro-simulation model, and concluded the potential benefits with integrated control at the corridor level. More recently, Tian (2007) proposed integrated ramp metering for diamond interchange control system based on the computed total delay occurring on the freeway mainline and its ramps, with a second-by-second analysis of the arriving and departure flow rates.

Overall, the existing studies of corridor congestion management have reported the necessity and effectiveness of integrating freeway access control with local arterial signal timing plans. Researchers working on this subject also share common concerns about the inevitable tradeoff between model accuracy and computing efficiency. Thus, how to

formulate an integrated corridor control model that is sufficiently reliable and efficient for real-time applications remains a challenging on-going issue for the community.

2.4   Freeway Access Control Strategies

Most studies of freeway access control focus on developing various on-ramp control strategies, which aim to keep the downstream freeway volume under the roadway capacity by limiting its on-ramp volume. Based on the employed logic, one can divide existing ramp metering studies into the following two categories: pretimed and automated control metering. Studies of the former sort use historical average volumes to compute the ramp metering rate, whereas those in the latter category focus on keeping traffic conditions near prespecified levels based on real-time traffic measurements. The automated metering strategies can use either actuated or adoptive control models, depending on the employed algorithm and the available data.

One pioneering study that used the linear programming method to produce the pretimed ramp metering rate was by Wattleworth (1963). The core idea of this study was to compute the volume on each freeway mainline segment using the historical average upstream volume and then to determine the on-ramp metering rate, with the control objective of maximizing the total entering flow rate within the freeway capacity constraints. Papageorgiou (1980) extended the same basic concept on formulating the interrelations between ramp flows and mainline flows with the linear programming method that incorporated a constant travel time for each freeway segment and produced the optimal metering rate with a decomposition approach. Similar studies alone this line, but with different objective functions, are also available in the literature (Yuan and Kreer; Tabac, 1972; Wang, 1972; Wang and May, 1973; Chen, Cruz et al., 1974; Chen, Cruz et al., 1974; Schwartz and Tan, 1977).

Note that pretimed ramp metering strategies aim to optimize ramp metering rates under stable traffic patterns. Hence, they often lead to underutilization of the freeway mainline capacity under time-varying traffic conditions.

In view the deficiencies inherent to all pretimed metering strategies, some researchers have proposed the use of automated metering strategies to optimize metering rates based on real-time measured traffic volumes and occupancies. Most of such studies

belong to one of the following categories: (1) local responsive control, where the ramp metering rate is determined solely by mainline traffic volumes on the adjacent freeway; and (2) coordinated ramp metering control, which computes the set of time-varying metering rates for ramps within the control boundaries, based on detected system-wide traffic conditions.

Example studies in the former category include the demand-capacity strategy by Masher, Ross et al. (1975); the zone-based control strategies by Stephanedes (1994); Xin, and Michalopoulos et al. (2004); and the congested pattern control approach by Kerner (2005). The demand-capacity strategy attempts to fully utilize the downstream capacity of the freeway mainline by reducing the ramp flow to its minimum level if the downstream occupancy becomes overcritical. This control algorithm follows an open-loop disturbance-rejection policy and is quite sensitive to disturbances caused by either traffic or measurement errors.

The zone-based control strategy, employed by the Minnesota DOT for many years, seeks to maintain a target level of traffic volume within each freeway zone, defined as a segment containing only one ramp. This strategy's effectiveness varies with the accuracy of the estimates for all associated control parameters, including the number of divided zones, the estimated bottleneck capacity, and the entering and leaving volumes of each zone over the control period. Xin et al. (2004) later extended this algorithm to stratified ramp control, which considers both the ramp demand and its queue size. The congested pattern control approach by Kerner (2005) employs a three-phase traffic flow concept to keep the on-ramp bottleneck at the minimum possible level that will not propagate its congestion patterns to upstream segments.

The occupancy-based control strategy determines the ramp metering rate based on the occupancy of the downstream freeway mainline, using feedback regulation to maintain a prespecified occupancy. Examples of occupancy-based strategies include ALINEA (Papageorgiou, Hadj-Salem et al., 1991), the neural control algorithm (Zhang and Ritchie, 1997; Xin, Michalopoulos et al., 2004), and the iterative-learning approach (Hou, Xu et al., 2008). The ALINEA algorithm proposed by Papageorgiou et al. (Papageorgiou, Hadj-Salem et al., 1991) is a closed-loop ramp metering strategy that uses classical feedback theory and dynamically adjusts the metering rates in response to

detected differences between the target and measured occupancies. The local artificial neural network model proposed by Zhang and Ritchie (1997) employs a multilayer feed-forward control structure, based on the fundamental diagram of traffic flow theory. Both ALINEA and neural control algorithms are reasonably effective for moderate congestion but not for heavy congestion, where queue spillback may occur. The core concept of the iterative-learning approach (Hou, Xu et al., 2008) is to formulate the density-based ramp metering control as an output-tracking and disturbance-rejection problem; this approach then employs an iterative learning algorithm along with the error-feedback method to yield a robust metering rate.

In view of the myopic nature of local control, some researchers have devoted tremendous efforts over the past decades to various coordinated metering strategies, including cooperative ramp metering, competitive ramp metering, and integrated ramp metering. An extensive summary of these strategies can be found elsewhere (Jacobson, et al., 1989; Nihan, 1991; Bogenberger, 1999; Zhang, et al., 2001). The literature includes some field experiments and extensive simulations of such strategies (Bogenberger, 1999).

The main control objective of a cooperative ramp metering system is to prevent the formation of both freeway mainline congestion and ramp spillback by adjusting the metering rate based on local traffic conditions and information about the spatial distribution of traffic volume over the entire system. The helper ramp metering algorithm by Lipp et al. (1991), which belongs to this category, consists of a local traffic-responsive metering algorithm and a centralized, coordinated operational override feature. The local responsive algorithm selects one of six predefined metering rates, based on each on-ramp's upstream mainline occupancy. If a meter rate reaches its critical status, the coordinated control begins to exercise its override function. The linked-ramp algorithm (Banks, 1993), another example in the same category, is based on the demand-capacity concept and uses the upstream volume to determine the local metering rate.

Unlike the cooperative metering models, the core logic of competitive algorithms involves computing two sets of metering rates based on both local and system-wide conditions and then implementing the more restrictive one to implement. The bottleneck algorithm (Jacobson, Henry et al., 1989) and the system-wide adaptive ramp metering

model (SWARM) (Paesani, Kerr et al., 1997; Ahn, Bertini et al., 2007) are two example studies in this category.

The bottleneck algorithm uses upstream occupancy data and bottleneck data to determine the metering rate for both a local ramp and the freeway bottleneck and then selects the more restrictive one. At the local level, it employs historical data to approximate the volume-occupancy relationships around capacity for each ramp. The local rate is set to be the difference between the estimated capacity and the measured upstream volume. To obtain the bottleneck metering rate, the algorithm first identifies bottlenecks and its volume reduction with the classical traffic flow theory, and then computes the bottleneck metering rate by distributing the reduced volume to upstream ramps with prespecified weights.

The SWARM algorithm also operates at two control levels. The local level computes the metering rate based on the local density and its system-wide reduction from ramps upstream of a critical bottleneck and then uses predetermined weights to distribute the volume to the upstream ramps. The algorithm identifies the bottlenecks based on the predicted, rather than measured, traffic conditions. Integrated ramp metering control directly generates metering rates from system-wide information. METALINE, the fuzzy local algorithm, and the coordinated artificial neural network algorithm belong to this category.

METALINE (Papageorgiou, 1990), an extension of ALINEA, is theoretically sound, but finding the proper control parameter matrices and the target occupancy vector is difficult. Fuzzy logic algorithms (Sasaki and Akiyama, 1986; Chen, May et al., 1990; Meldrum and Taylor, 1995; Taylor, Meldrum et al., 1998) convert empirical knowledge about ramp control into fuzzy rules. The effectiveness of such control algorithms depends on the accuracy of the embedded fuzzy rules derived from empirical data. The coordinated artificial neural network algorithm (Wei and Wu, 1996) divides the freeway segment under control into several zones and computes the metering rate based on the collected volume-to-capacity ratios upstream and downstream of the ramp and the queue length within each zone.

One common feature of all adaptive ramp metering algorithms is that they explicitly specify an objective function, such as minimizing total travel time, maximizing

system throughput, etc., to govern the selection of metering rates for all ramps within the control boundaries. The Hanshin algorithm by Yoshino et al. (1995) pioneered the use of such algorithms. They employed a linear programming model to maximize the total number of vehicles entering the system while preventing traffic congestion in any segment of the expressway and the surrounding road networks. Lovell and Daganzo (2000) proposed an improved time-dependent control strategy for freeway networks with bottlenecks and a computationally efficient greedy heuristic algorithm for solving the metering rate. Recognizing the complexity of model formulations and the difficulty in obtaining real-time OD information, Zhang and Levinson (2004) formulated a similar linear program that uses only variables directly measurable from detectors. Gomes and Horowitz (2006) also presented a similar linear control model, but used the asymmetric cell transmission method (ACTM) to minimize the total freeway travel time.

The dynamic metering control algorithm by Chen et al. (1997) represents another cluster of studies. This algorithm generally consists of four operational elements: state estimation, OD prediction, local metering control, and area-wide metering control. At their core, such algorithms form a hierarchical structure with a local feedback control module (ALINEA) and a system-wide control model. The latter employs a linear-quadratic feedback control to produce nominal metering for local controllers, which then compensate the nominal set of metering rates based on the detected local traffic disturbances and prediction errors.

The linear-quadratic (LQ) feedback control algorithm is one of the most commonly studied methods within the automatic control theory for coordinated freeway ramp metering (Yuan and Kreer, 1971; Kaya, 1972; Papageorgiou, 1983; Payne, Brown et al., 1985; Papageorgiou, Blosseville et al., 1990). The key logic of such LQ feedback strategies is to convert the nonlinear traffic state equations around a certain desirable trajectory, employing a quadratic penalty function in the objective function to represent the state and control deviations from the desired trajectory.

The successive optimization algorithm represents another school of methods for solving the ramp metering rates for large-scale networks. Chang et al. (1994) presented such an algorithm to solve the complex control model that captures the dynamic evolution of traffic with two-segment linear flow-density relationships. An example

application of such a model with a rolling time horizon for freeway corridors can be found in the literature (Wu and Chang, 1999).

In summary, ramp metering is one of the most direct and efficient means to mitigate freeway local congestion if appropriately implemented. The benefits include an increase in freeway mainline throughput and a reduction in travel time or delay. However, these are achieved at the cost of excessive on-ramp queues, which may spill back and block neighboring urban arterials (Levinson and Zhang, 2006). To achieve better performance for the entire corridor, the control boundaries should include both the freeway and its neighboring arterials.

2.5   Arterial Traffic Signal Control Strategies

Signal control is an essential control strategy used to increase arterial capacity and to mitigate daily congestion. Webster and Cobbe (1967) first introduced a formula to optimize the signal timing plans for an isolated intersection. Building on Webster's work, some researchers later proposed pretimed signal control models that employed phase-based strategies to optimize the splits, cycle length, and phasing in order to minimize the total delay. Examples of such studies are SIGSET (Allsop, 1971) and SIGCAP (Allsop, 1976). SIGSET applied Webster's nonlinear total delay function for undersaturated conditions (1958) as the objective function and imposed some linear constraints on key control parameters. SIGCAP is mainly used to minimize delay for multiple demand patterns under the same constraints. A similar model, but using the binary-mixed-integer programming method, also appeared later in the literature (Improta and Cantarella, 1984). Some researchers have extended the core concept of SIGCAP to formulate a so-called reserve capacity model (Wong and Yang, 1997; Wong, Wong et al., 2007).

All of the aforementioned example models are used only to control undersaturated, isolated intersections, neglecting the interrelationships of traffic flow evolution between intersections. Hence, optimizing the progression of all intersections in the same arterial emerged as a popular research subject (Morgan and Little, 1964). One pioneering study by Little et al. (1966; 1981) following this line of inquiry proposed the use of mixed-integer linear programming. Their model, named MAXBAND, aimed to optimally time the red light durations of all signals on the same arterial so as to maximize

its inbound and outbound progression bandwidths. This mixed-integer linear programming model was solved with the traditional branch-and-bound algorithm; later, Chaudhary et al. improved its efficiency (1991). Several researchers later extended this pioneering arterial model to multiband phasing plans, including optimizing the left-turn phase sequence (Chang et al., 1988), the weighted bandwidth for each directional road section (Gartner et al., 1991; 1996), and the time-varying demand conditions (Han, 1996).

Instead of maximizing the progression band, TRANSYT (Robertson, 1969) offered an alternative signal control objective of minimizing a performance index consisting of prespecified MOEs, such as delay, number of stops, or queue length. This signal design software is one of the most popular programs among both the research and application communities, and its results are often used as the baseline for evaluating various new signal control strategies (Papageorgiou, Diakaki et al., 2003). The core logic of TRANSYT was used later in a responsive signal network control system, SCOOT (Split, Cycle, Offset Optimization Technique) by Hunt et al. (1982).

Note that, due to the emergence of sensor technologies and to the necessity of responding to traffic conditions in real time, the focus of traffic control researchers has evolved from optimizing pretimed arterial signals to developing real-time adaptive or semi-adaptive systems. Some popular real-time signal control systems include: SCAT (Sims and Dobinson, 1980), OPAC (Gartner, 1983), PRODYN (Henry, Farges et al., 1984), CRONOS (Boillot, Blosseville et al., 1992), RHODES (Sen and Head, 1997), and ARTC (Kim, Liu et al., 1993). The advent of intelligent transportation systems has turned the design and implementation of these real-time control systems into a popular task. Their effectiveness in contending with saturated traffic conditions and the resulting costs and benefits, however, remain on-going research issues.

2.6   Signal control models for oversaturated conditions

Oversaturation refers to conditions where traffic queues persist from one cycle to the next, due either to insufficient green splits or to lane-blockage. In such conditions, traffic queues along signalized arterials may block upstream intersections, thus exacerbating already congested conditions. Gazis et al. (1963) were the pioneer

researchers who employed a graphic method to optimize two closely spaced and oversaturated intersections.

In 1997, Abu-Lebdeh and Benekohal (1997) developed an algorithm to optimize the signal timing for oversaturated arterials with a queue polygon approach, which assumed the existence of a continuous queue and a link blockage. They later extended their proposed GA-based solution to include a disutility function for evaluating a variety of traffic management scenarios (Abu-Lebdeh and Benekohal, 2000, 2003). Along the same lines, Abu-Lebdeh, et al. (2007) further developed several models that could capture the interactions of traffic streams between neighboring lanes and among successive signals under oversaturated traffic demand levels.

In the same vein, Chang and Lin (2000) analyzed queue evolution at an isolated intersection cycle by cycle, based on the assumptions of a constant arrival rate and the continuous formation of the traffic queue. Their study employed two objective functions: one, in a quadratic form, was for the delay of each cycle during the entire oversaturated period; the other, a performance index, accounted for the total delay and stop penalty. Chang and Sun (2004) later extended this model to optimize an oversaturated signalized network.

Hadi and Wallace (1995) proposed an enhancement function to TRANSYT-7F that could optimize signal-timing plans under congested conditions. TRANSYT-7F, Release 8 (Li and Gan, 1999) also offers a function to model link spillback and lane blockage by reducing the corresponding link saturation flow. For the same oversaturated intersection, Park, Messer et al. (1999) employed the queue polygon method to compute the queue delay and to track the link blockage by continually checking the end-of-queue vehicle. They proposed preliminary and enhanced solution algorithms based on the lore logic of GAs (Park, Messer et al., 2000).

CHAPTER 3: OVERALL SYSTEM FRAMEWORK

3.1 Introduction

This chapter presents the overall structure of the proposed integrated off-ramp control system for managing recurrent congestion under various traffic conditions. This chapter also focuses on the interrelationships between its principle components, along with critical control factors and underlying assumptions.

The remaining sections of this chapter are organized as follows: Section 3.2 presents the major research issues and challenges involved in developing a system capable of contending with recurrent congestion at urban freeway interchanges, including off-ramp overflow, on-ramp queue spillback, and intersection lane blockage. Section 3.3 illustrates the control flowchart of the proposed integrated control system, based on the research scope and intended applications.   Finally, Section 3.4 discusses the proposed functions for each principle control component and their operational interrelationships.

3.2 Key Research Issues

The proposed system aims to maximize the operational efficiency of congested urban interchanges. Given the research objectives and the required system functions stated in Chapter 1, the development of such a system must first address the following major research issues:

- How to capture the interactions of traffic patterns that include lane and link blockages as they evolve from moderate congestion to oversaturated conditions;

- How to model the complex interrelationships between traffic queues on on-ramps, off-ramps, and freeway mainline segments at various congestion levels.

- How to balance the delays between freeway and arterial vehicles to achieve the optimal state for the entire system;

- How to formulate all of the identified complex interactions between both freeway ramp and arterial traffic flows and their evolving patterns with an

integrated signal-ramp control model that can yield effective and reliable solutions for real-time applications; and

– How to contend with the occurrence of traffic measurement errors and still yield robust solutions for field operations.

To handle the above issues, we have divided the research into the following tasks:

Task 1: Modeling the interrelationships between the off-ramp queue and lane blockages at neighboring intersections, as well as on-ramp spillback at various congestion levels. This task will contend with recurrent congestion patterns in which saturated local traffic conditions may cause the formation of off-ramp queues without affecting the operational capacity of the mainline segment.

Task 2: Formulating an integrated interchange control model that can account for the trade-off between delays on local arterials and the freeway mainline, yielding optimal system-wide congestion control. The proposed model should concurrently optimize the on-ramp and off-ramp metering plans, as well as signal timing plans for the adjacent local arterials.

Task 3: Developing a generalized interchange control model to contend with recurrent or nonrecurrent congestion scenarios where off-ramp queue may spill back into the freeway mainline and interfere with the merging traffic flow from one or more upstream ramps. This task will tackle the severe congestion pattern where both the freeway and local arterial are oversaturated and the off-ramp queue may significantly reduce the mainline capacity, spilling back to upstream ramps.

Task 4: Designing efficient solution algorithms for both the base model for off-ramp control and the extended model for integrated interchange system optimization. The proposed algorithm will be capable of generating efficient control parameters in response to information deficiencies and dynamic traffic flow interactions between the freeway and arterials at various congestion levels.

Task 5: Evaluating the effectiveness of the proposed models with extensive numerical experiments and field tests. The primary focus of this task is to ensure the applicability of the proposed system to the target I-495 interchange, which often

experiences off-ramp queue spillback during daily commuting hours. We will use extensive numerical experiments, along with traffic scenarios observed in the field, to assess the potential and constraints of implementing the proposed integrated control system under various traffic conditions.

3.3   System Control Structure and key modules

To ensure that the results from each of the above tasks can be integrated into a seamless control structure and can be activated based on the detected congestion level, this study has developed an overall control architecture for the proposed system with the following three levels:

Level 1: The off-ramp queue spills back to the freeway mainline. The control action for such a scenario will consider the mainline traffic delay in optimizing the signal timings at the off-ramp and intersections on the neighboring arterial.

Level 2: The on-ramp queue spills back to its upstream intersection. Note that an insufficient metering rate may cause the queue vehicles to block one or more arterial through lane(s), consequently causing the through traffic to spill back to upstream intersections if the arterial through demand is larger than its remaining capacity. The control strategy at this level will activate its oversaturated intersection module to maximize the total throughput within the control boundaries.

Level 3: The freeway mainline in the interchange area experiences a moving queue and spills back to the upstream interchange. This level of control is designed for congestion scenarios where both freeway and local arterial volumes at the interchange have reached the saturation level. The on-ramp queue has spilled back to nearby arterial through lanes, and the off-ramp vehicles have propagated to the freeway mainline lanes and to an upstream on-ramp.

Model Inputs

Traffic demand

Signal Timing & ramp metering timing

Traffic Control Models

Off-ramp spillback check

On-ramp spillback check

Off-ramp spillback?

Yes

No

On-ramp spillback?

Yes

On-ramp spillback check

Integrated on-ramp control

Yes

No

On-ramp, off-ramp, and signal operated separately

On-ramp spillback?

No

Yes

Freeway mainline spillback check

Integrated off-ramp control

No

Single interchange integrated control

Spillback to upstream?

No

Yes

Multi-interchange integrated control

Model Outputs

- Signal timings
- Ramp metering timings
- Traffic MOEs
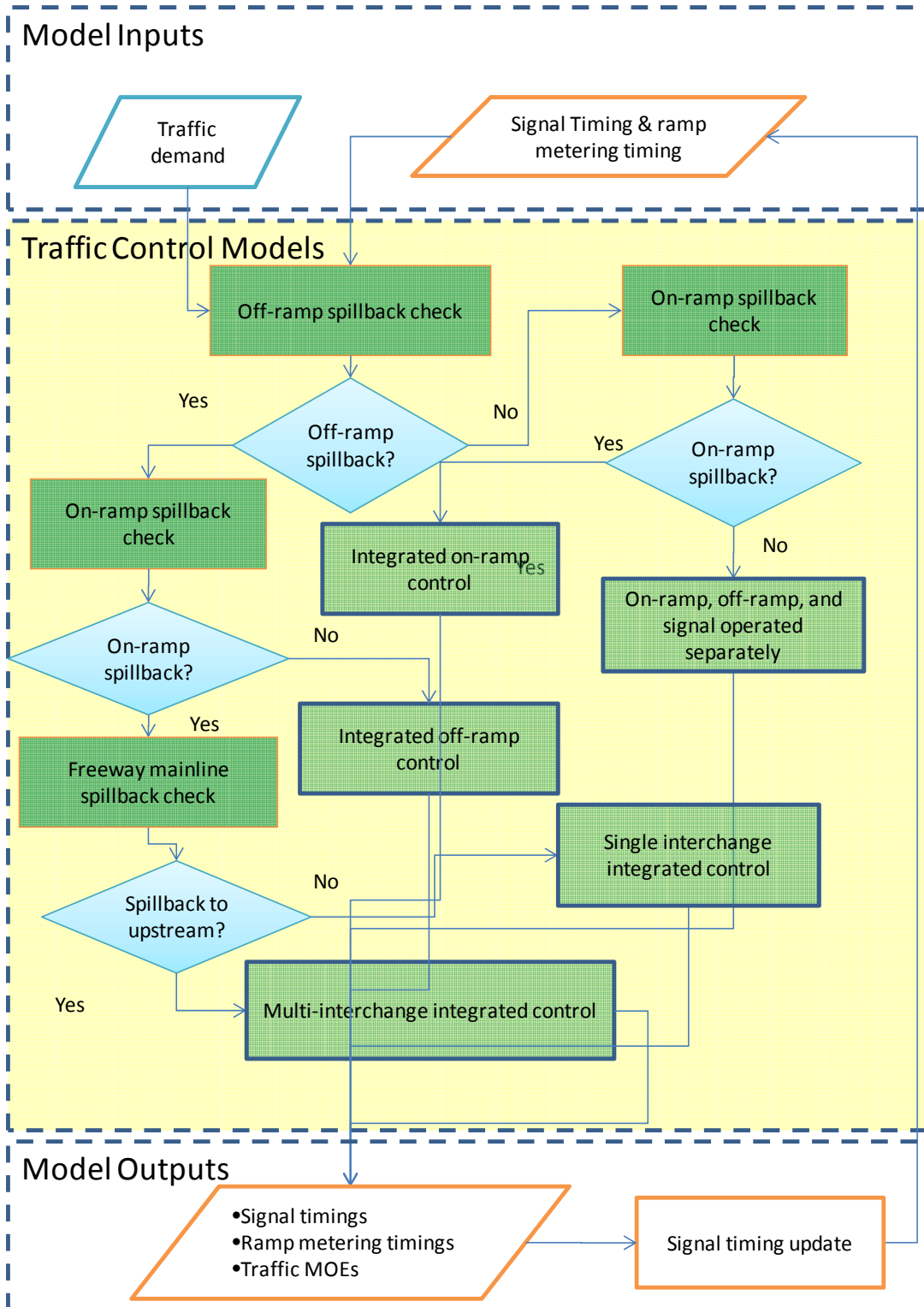
Signal timing update

Figure 3-1 System Control Flowchart

Figure 3-1 illustrates the feedback control process for system operations of the proposed integrated interchange control model, which takes traffic demand and the existing signal timing as inputs and then executes the simulation model to check whether or not queue spillback is occurring at on- and off-ramps.

On-ramp metering and arterial signals (including off-ramp signals) will be operated independently if neither experiences any queue spillback. If queue spillback occurs only at off-ramps, the system will execute the off-ramp integrated control model to maximize system performance. Likewise, if only on-ramps exhibit excessive queues, the proposed system shall activate just the on-ramp control model to balance freeway and arterial delays. Conceivably, all modules in the proposed integrated system would be activated if both on-ramps and off-ramps were suffering from long queue spillbacks. The simulation module would also check freeway mainline spillback and would execute the multi-interchange model to coordinate all control plans activated at the two neighboring interchanges.

Note that the entire system illustrated in Figure 3-1 requires various inputs for its online operations, including

- Roadway geometric features, such as the number of ramps; the distance between ramps and intersections; and the lengths of the left-turn bay, the deceleration lane, and the on-ramp acceleration lane;

- Traffic volumes on the freeway's mainline and ramps, as well as on the arterials and their intersections;

- Turning proportions at both neighboring intersections and off-ramps;

- Operational constraints for signal timing and metering plans; and

- Traffic flow parameters that reflect local driving characteristics.

To provide the aforementioned operational functions in response to various levels of saturated and oversaturated traffic congestion, the proposed integrated interchange control system has the following modules: an arterial signal timing optimization module, an off-ramp integrated control module, an on-ramp integrated control module, a single-

interchange integrated control module, and an extended interchange control module. The interrelationships between those modules are illustrated in Figure 0-1.

Note that the arterial signal timing module aims to optimize the cycle length, offset, and green split for all signals within the control boundaries under both under- and oversaturated conditions. The proposed module has the capability to take into account the blockage between lanes and spillback between intersections.

The off-ramp integrated control module will incorporate ramp queue delay and its impact on freeway mainline traffic into the arterial signal timing module to ensure the proper balance between these two roadway systems. The on-ramp integrated control module will extend the functions of the local arterial signal optimization module and concurrently account for on-ramp flow delays in the system-wide signal control process. All of the aforementioned modules with a prespecified overall control objective naturally form the single-interchange integrated operational module.

The single interchange control system can be extended to cover multiple interchanges if the freeway queue, due to both heavy mainline volume and off-ramp spillback, reaches upstream on-ramps. Effectively controlling such congestion patterns, however, is a much more complex problem: the performance of the entire traffic system must be maximized from the corridor management perspective, and potential detour routes might also require identification to balance the traffic volume between the primary commuting freeway and alternative routes. Since the compliance of drivers with control strategies and guidance information is one of the most critical issues determining the effectiveness of corridor-level operational strategies, we propose leaving the study of such an extension for a future project.
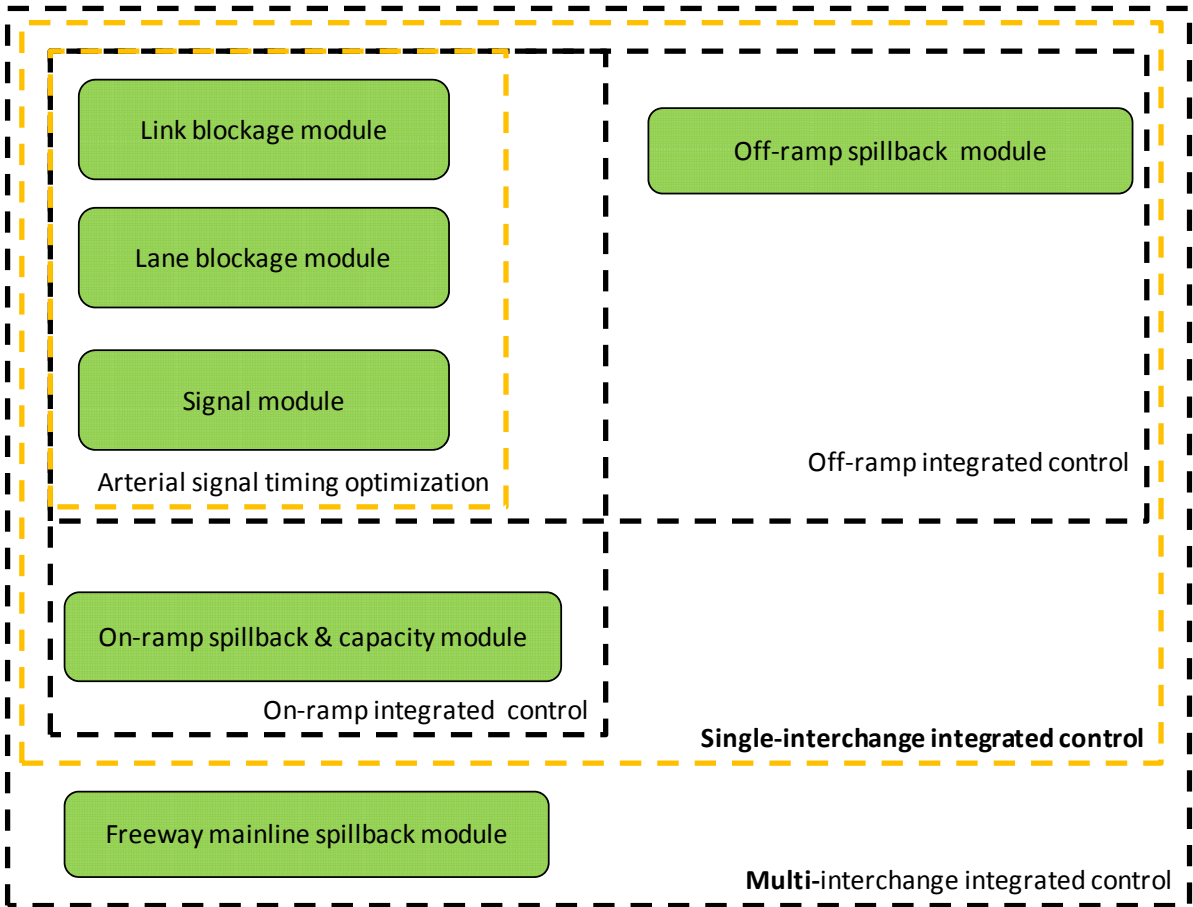
Figure 0-1 Key System Modules

CHAPTER 4: ARTERIAL TRAFFIC FLOW AND SIGNAL MODELS

4.1   Introduction

This chapter presents the methodology for modeling the complex traffic flow interactions between intersections and the potential blockage between neighboring lanes due to oversaturated demand. Its focus is on formulations for signal optimization and the control process under different congestion levels. Since queue spillback and its resulting blockage to through movements often occur on local arterials receiving off-ramp flows from congested interchanges, the model formulations detailed in this chapter offer the foundation for developing an integrated arterial signal optimization system that can take full account of the channelization effects on turning traffic and to capture the movement blockage between lanes.

The remaining sections of this chapter are organized as followings: Section 4.2 will discuss the modeling methodology for arterial traffic dynamics under oversaturated traffic conditions. Section 4.3 will focus on the signal optimization model and a GA-based solution algorithm. Section 4.4 will report conclusions.

4.2   Modeling Traffic Flow Interactions at Signalized Intersections

To model the temporal and spatial interactions of traffic flows at a signalized intersection, one can conceptually divide each link into the following four zones: the merging, propagation, diverging and departure zones (see Figure 4-2). Vehicles entering such a link will move over these four zones and then bound to their respective destinations. Notably, vehicles for left-turn and through movements could block each other due to spillback if the bay length and signal timings are not adequate for the time-varying traffic volume. The traffic queue caused by lane-blockage could spill back to upstream intersections under oversaturated traffic conditions.
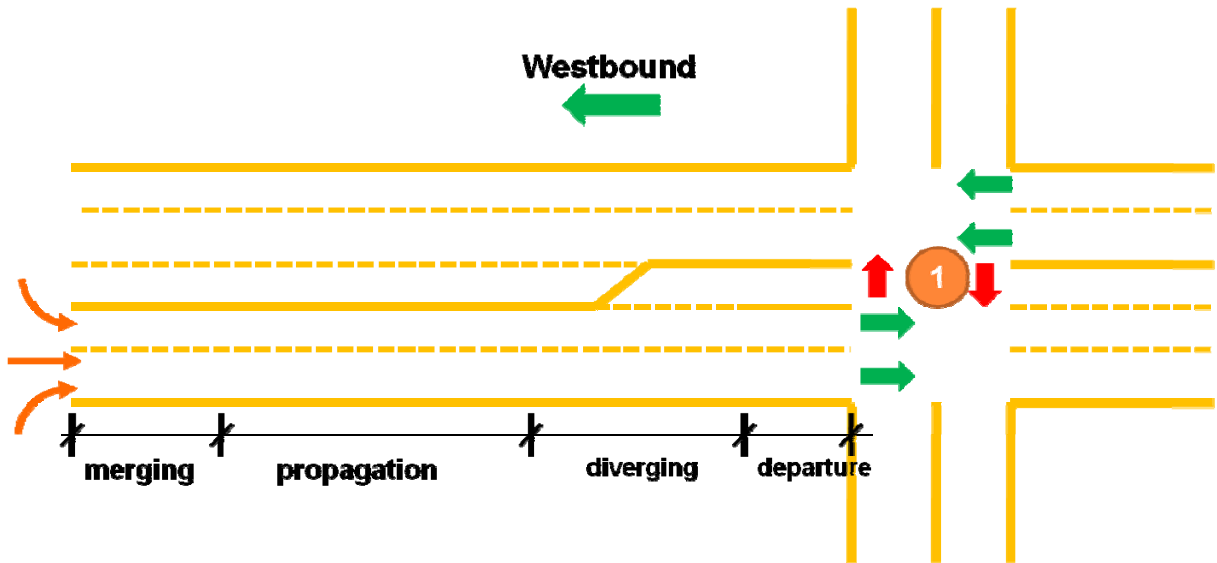
Figure 4-2 The traffic dynamic of a signalized intersection approach

To optimize the signal plans for arterials experiencing lane-blockage conditions at some intersections, this study first employs the Cell Transmission concept (CTM) by Daganzo (1994, 1995b) to formulate the flow interactions in the above four zones. CTM is a finite difference approximation of the traffic flow model by Lighthill and Whitham (1955) and Richards (Richards 1956). Its core concept is to divide the target roadway into a number of homogeneous sections (named cells), and each has its length equal to the distance traveled by a vehicle at the free-flow speed during one unit time interval.

Any model developed with CTM can track the states of the traffic system at any time instant by the number of vehicles in each cell, denoted as n_i^t. In addition, CTM employs the following commonly-used parameters in representing the key traffic flow variables, where time t represents the time interval $[t, t+1]$:

- N_i^t is the buffer capacity, defined as the maximum number of vehicles that can be presented in cell i at time t, which is the product of cell length multiplied by the jam density;
- Q_i^t is the flow capacity in time t, defined as the maximum number of vehicles that can flow into cell i, which is the product of the cell's saturated flow multiplied by the length of time interval;
- y_{ij}^t defines the number of vehicles leaving cell i and entering cell j at time t.

30

Any CTM model generally consists of three types of cells: the ordinary cell, the merging cell and the diverging cell. The ordinary cell can have only one upstream and one downstream cells; the merging cell has multiple upstream cells but one downstream cell; the diverging cell can have only one upstream cell but multiple downstream cells. The following two expressions illustrate the recursive relationships between these three types of cell:

$$n_i^{t+1} = n_i^t + y_{i,in}^t + y_{i,out}^t \qquad (4\text{-}1)$$

$$y_{i,in}^t = \sum_{k \in \Gamma(i)} y_{ki}^t, \; and \; y_{i,out}^t = \sum_{j \in \Gamma^-(i)} y_{ij}^t \qquad (4\text{-}2)$$

Equation (4-1) represents the flow conservation relationship at the cell level, which means that the number of vehicles within a cell in the next time interval equals the vehicle number of this interval and the difference between all entering and departing vehicles. The second and third terms in Equation (4-1) vary with the cell category, where y_{ij}^t needs to be computed with a traffic flow-density relationship.

To represent the complex traffic behavior such as lane-blockage, it is necessary to track the vehicle number for each movement. Thus, this study employs the following recursive relationship at the movement level for each cell, in additional to the flow conservation at the cell level:

$$n_{i,m}^{t+1} = n_{i,m}^t + y_{i,m,in}^t - y_{i,m,out}^t \qquad (4\text{-}3)$$

where $n_{i,m}^t$ is the vehicle number for movement m of Cell i; $y_{i,m,in}^t$ is the number of those vehicle that travel from upstream cell (i.e., Cell s) to Cell i and will stay in the movement m of Cell I; and $y_{i,m,out}^t$ is the number of vehicles that depart from movement m of Cell i.

4.2.1 Merging zone

In the merging zone, vehicles from different upstream approaches will join together to form a new traffic stream. During oversaturated traffic conditions, the large volume of vehicles from this aggregate traffic stream could cause long queue spillback and thus block the upstream traffic as shown in Figure 4-3.
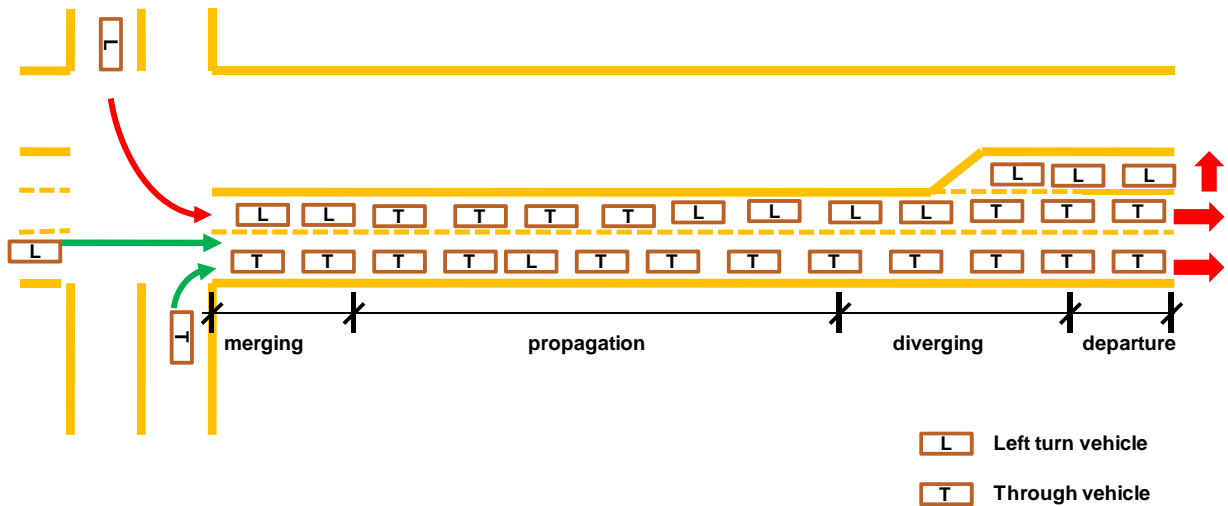

Figure 4-3 Link spillback blockage at the merging zone

The merging cell is best suited for modeling the traffic flow interactions in the merging zone. As illustrated in Figure 4-4, Cell-C represents the merging zone; Cell-A, Cell-B, Cell-D represent the upstream through, right-turn, and left-turn approaches. At signalized intersections, since upstream vehicles will be given different priorities to enter the merging zone based on the signal phasing plan, one can then use Equations (4-4) to capture their relationships.
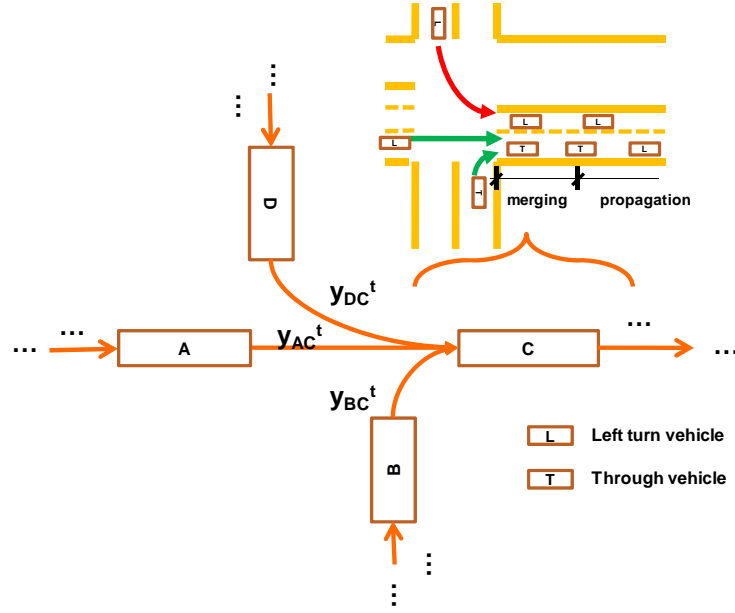
Figure 4-4 The merging zone represented by a merging cell

$$y_{iC}^t = \min\{n_i^t, Q_i^t, \delta[N_C - n_C^t]\}, i = A, B, D \tag{4-4}$$

Where $\delta = 1, \text{if } n_i^t \leq Q_i^t$, and $\delta = -\frac{w}{v}, \text{if } n_i^t > Q_i^t$ in which w represents the backward propagating speed of the disturbances and v is the free-flow speed. When the merging zone represented by Cell-C is full (i.e., the vehicle number in Cell-C, n_C^t, equal its buffer capacity, N_C^t), no vehicle can enter the merging zone (i.e., $N_C^t - n_C^t = 0$ which implies $y_{iC}^t = 0$).

Hence, with the given turning percentage from each movement, one can update the number of vehicles for each movement during each time interval with the following expression:

$$y_{C,m,in}^t = r_{lm}^t\left(\sum_i y_{iC}^t\right), i = A, B, D \text{ for each movement } m \tag{4-5}$$

Where r_{lm}^t denotes the percentage of vehicles joining each movement; l, m represent the link identity number and movement, respectively.

4.2.2 Propagation zone

In the propagation zone, the interactions between vehicles increase with the traffic volume. From the aggregate perspective, the flow-density relationship can best represent such interactions. Hence, to compute the optimal signal plan for an arterial, one needs to realistically formulate the temporal and spatial relations of vehicles evolving over the link between neighboring intersections.
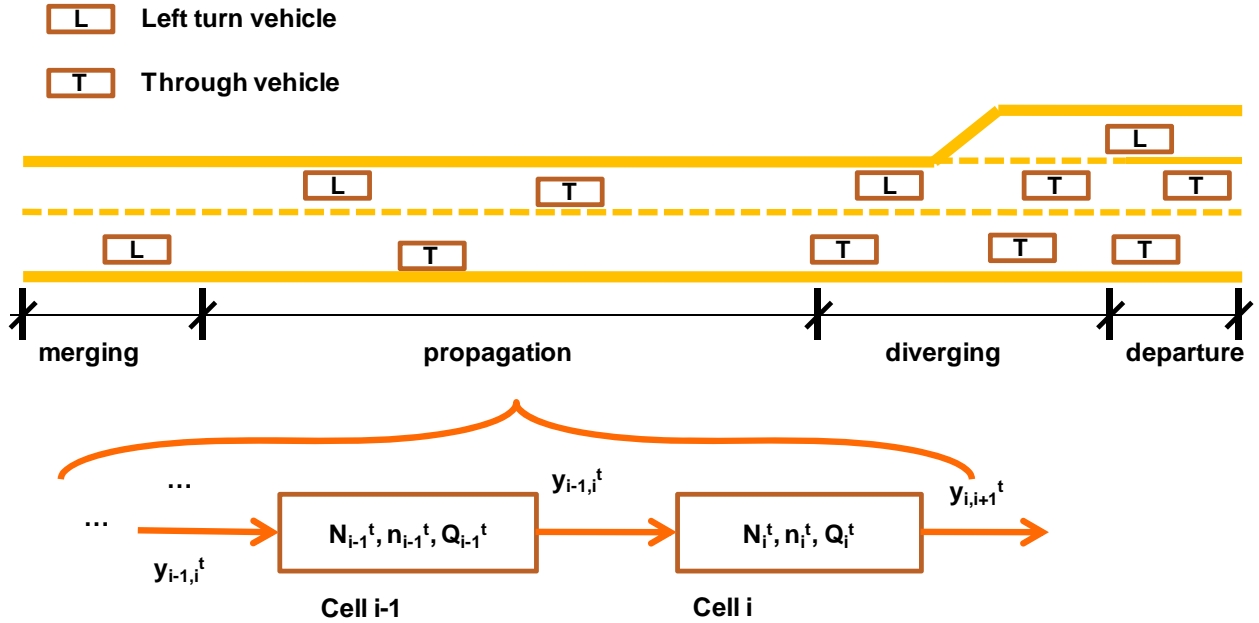
Figure 4-5 The propagation zone represented with ordinary cells

To tackle this issue, this study employs the ordinary cell to capture this type of vehicle interactions in the propagation zone. As illustrated in Figure 4-5, the number of cells in the propagation zone may vary with the link length. Each ordinary cell has one upstream cell and one downstream cell. Equation 4-6 computes the number of vehicles exiting cell i and entering cell i+1 in time t ($y_{i,i+1}^{t}$), a simplified flow-density relationship proposed by Daganzo (1956) to capture the traffic dynamics under various traffic conditions.

$$y_{i,out}^{t} = y_{i+1,in}^{t} = \min\{n_i^t, Q_i^t, \delta[N_{i+1} - n_{i+1}^t]\}$$

(4-6)

If one defines $S_i^t (= \min\{Q_i^t, n_i^t\})$ as the sending capacity, and $R_i^t (= \min\{Q_i^t, \delta(N_i^t - n_i^t)\})$ as the receiving capacity of cell i, then Equation (4-6) naturally evolves to Equation (4-7).

$$y_{i,i+1}^t = \min\{S_i^t, R_{i+1}^t\} \tag{4-7}$$

$$y_{i,m,out}^t = y_{i,out}^t \times \frac{n_{i,m}^t}{n_i^t} \ \textit{for each movement } m \tag{4-8}$$

4.2.3   Diverging zone – a new set of formulations

In the diverging zone, vehicles bound to different destinations may have to join different queues in order to be at their target movements. Hence, under oversaturated conditions, it is likely to incur blockage between different movements due to queue spillback in some movements. For instance, depending on the bay length and its incoming volume, the left-turn queue could spill back to block the through traffic.

Note that although there are several different types of lane blockage at an oversaturated intersection, the presentation hereafter will focus only on the formulations for interaction between left-turn and through vehicles. One can apply the identical concept to model all other types of blockage between lanes. Figure 4-5 and Figure 4-6 show two possible types of blockage between left-turn and through lanes at an intersection.

L   Left turn vehicle
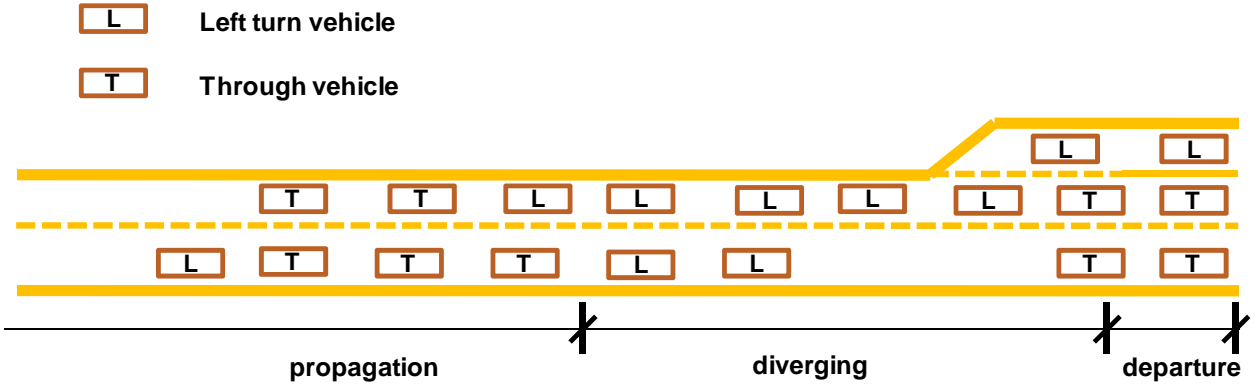
T   Through vehicle

Figure 4-6 Left-turn vehicles block through traffic

L   Left turn vehicle

T   Through vehicle

propagation   diverging   departure
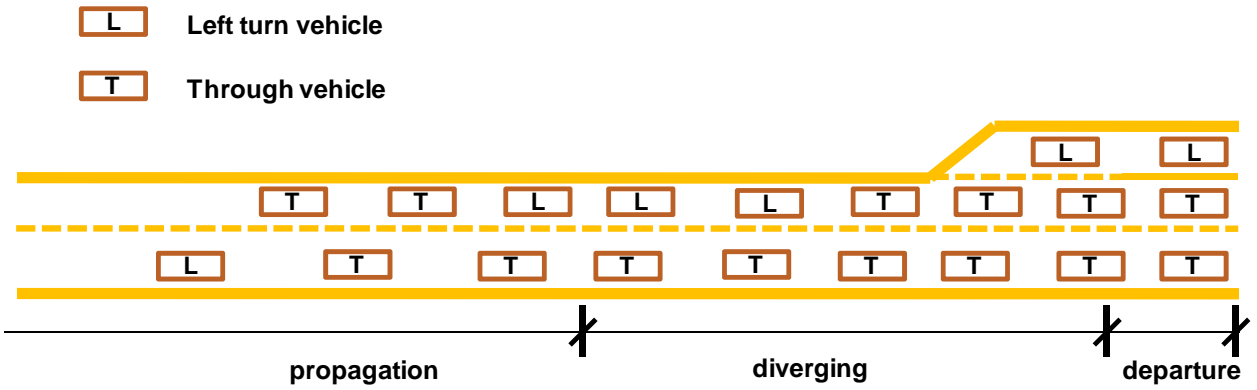
Figure 4-7 Through vehicles block left-turn traffic
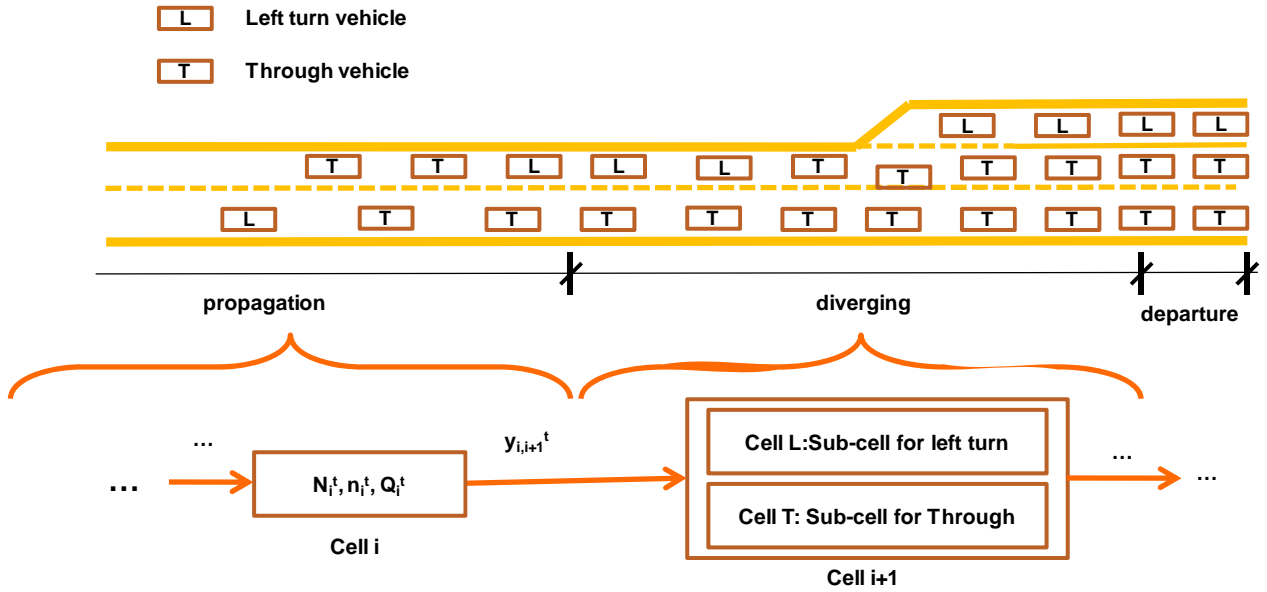
Figure 4-8 The sub-cell concept illustration

To realistically capture these two types of queue and lane blockage effect on neighboring movements, this study proposes a sub-cell modeling concept, an enhancement to the existing CTM methodology. Figure 4-8 illustrates the use of the proposed sub-cell concept to the diverging zone link that consists of a diverging cell, Cell i+1, which has two sub-cells: sub-cell L for left-turning vehicles and sub-cell T for through traffic.
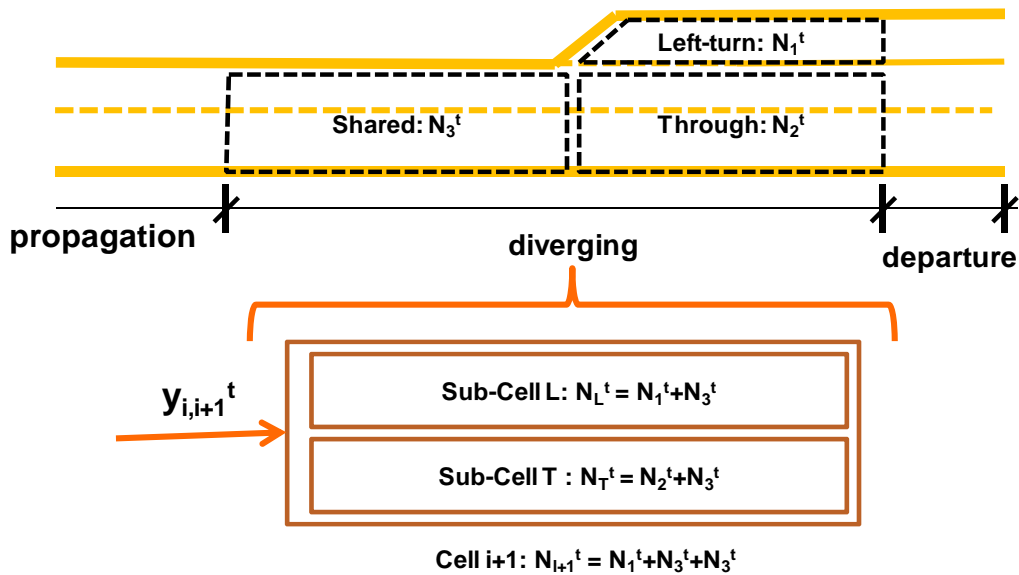
Figure 4-9 The sub-cell representation of a diverging signalized cell

Figure 4-8 illustrates the use of three sub-zones to model the vehicle interactions in the diverging zone, where Zone 1, denoted by N_1^i, is the space exclusively for left-turn traffic; Zone 2, N_2^i, is the space only for through traffic; and Zone 3, N_3^i, is the space to share by left-turn and through traffic. Equations (4-9) and (4-10) presented below are for computing the buffer capacity of each sub-cell:

$$N_L^i = N_1^i + N_3^i$$

(4-9)

$$N_T^i = N_2^i + N_3^i$$

(4-10)

$$N_{i+1}^i = N_1^i + N_2^i + N_3^i$$

(4-11)

 Equation (4-11) captures the physical buffer capacity of diverging cell *i+1*. Note that one can divide these zones based on the channelization at the signalized approach. The buffer capacity of these sub cells explicitly reflects the turning bay effect. One can compute the flow capacity of each sub-cell, based on its number of lanes and the saturation flow rate.

Based on the above definitions, the study presents the following linear programming formulations to represent the time-varying status of such sub-cells:

$$max \sum_m y_{i,m,out}^t$$

(4-12)

$$\sum y_{i,m,out}^t \le R_{i+1}^t$$

(4-13)

$$y_{i,m,out}^t \le \delta(N_{i,m}^t - n_{i+1,m}^t)$$

(4-14)

$$\sum y^t_{i,m,out} \leq S^t_i \tag{4-15}$$

$$y^t_{i,m,out} \leq S^t_i \times \frac{n^t_{i,m}}{n^t_i} \tag{4-16}$$

$$y^t_{i,m,out} \leq Q^t_{i,m} \tag{4-17}$$

Equation (4-12) assumes that drivers always intend to fully utilize the available capacity and space. For instance, as shown in Figure 4-10, when the left-turn queue spillback occurs, the coming left-turn vehicles will inevitably occupy all the shared zone space if the volume continues to increase.
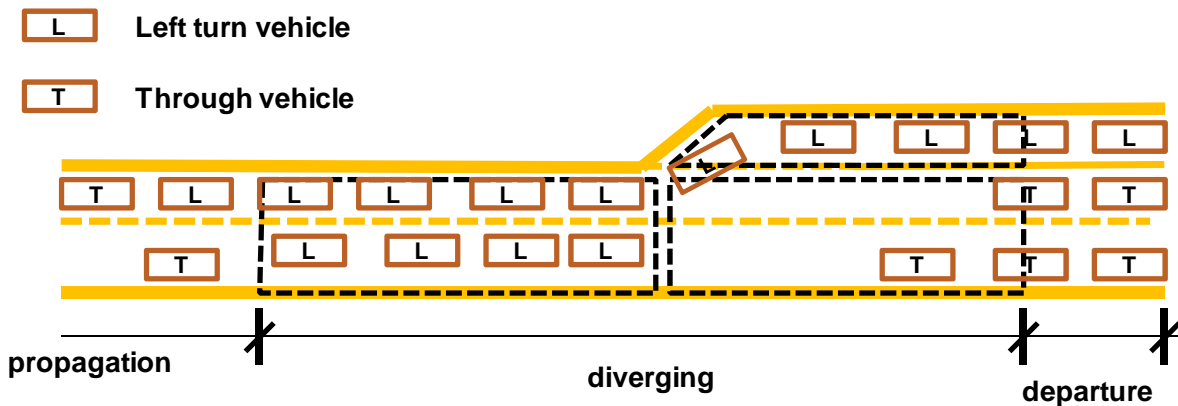
Figure 4-10 An example illustration of left-turn queue blocking through traffic

The new diverging model developed in this research can explicitly reflect the effect of the turning bay, and capture some lane blockage relations with Equations (4-12), (4-13), and (4-17). The third term in the parenthesis of Equation (4-12) is the minimum of these three terms, which implies $w^t_i = R^t_L / r^t_L$. By substituting it into Equations (4-13) and (4-17), it leads to the following results: $y^t_{iL} = R^t_L$ and $y^t_{iT} = R^t_L \times r^t_T / r^t_L$. If R^t_L decreases, y^t_{iL} and y^t_{iT} will also decrease. When $R^t_L = 0$, it indicates that left-turn vehicles have blocked through traffic completely. In the scenario

of through blocking left-turn traffic, one can perform the same analysis to formulate their relationships.

The segment in the departure zone is modeled with a signalized cell, and its flow capacity Q_i^t is defined as follows:

$$Q_i^t = Q_{i,max} \, g_i^t \qquad (4\text{-}18)$$

where g_i^t is the green time in time interval t.

4.2.4   An Optimization Model for Oversaturated Arterial Signal

Objective functions

Depending on the traffic conditions, one can set the control objective function as maximizing the total system throughput or minimizing the total delay. Using the above formulations, this study has set the objective function of maximizing the system throughput as follows:

$$Max \ \ (Throughput = \sum_{t=0}^{T} \sum_{j \in S} \sum_{i \in \Gamma^-(j)} y_{ij}^t) \qquad (4\text{-}19)$$

where S is the sink cell set; $\Gamma^-(j)$ is the upstream cell set of cell j; and T is total operating time period.

In CTM, the length of each cell is set to be the free-flow travel distance over a pre-specified unit, which means that the vehicles at each unit time in each cell can either stay or move to the downstream cells. Hence, one can approximate the delay as the difference between a vehicle's actual and its free-flow travel times over a given distance. For instance, if some vehicles staying in the same cell over n consecutive unit intervals, then it implies that they have experienced n unit delay times.

More specifically, one can define the delay over each cell for time interval t as $d_i^t = \left(n_i^{t-1} - \sum_{j \in \Gamma(i)} y_{ij}^t \right) \times \tau$, where $\Gamma(i)$ is the downstream cell set of cell i and τ is

the time period length. Thus, one can propose an alternative objective function of minimizing the total system delay as follows:

$$Min\ [total\ delay = \quad \tau \sum_{t=0}^{T} \sum_{i} (n_i^t - \sum_{f \in \Gamma(i)} y_{if}^t]$$

(4-20)

As T is a constant, the objective function of minimizing the system delay can is identical to the follow expression:

$$Min\ [total\ delay = \quad \sum_{t=0}^{T} \sum_{i} (n_i^t - \sum_{f \in \Gamma(i)} y_{if}^t]$$

(4-21)

4.1.1 Signal timing operation

Figure 4-11 illustrates a typical four-leg intersection and the NEMA (National Electrical Manufacturers Association) eight-phase structure, where the right-turn on red is assumed to be permitted.

Using the NEMA phase system has two advantages: (1) it can model all possible phases for a signal by switching the sequence of some provided phases (see Figure 4-11); and (2) it offers the flexibility to accommodate exclusive left-turning traffic with the leading-lagging phases. Hence, through the sixteen NEMA phases, one can find the optimal one from all possible combinations of the candidate signal phasing plans.
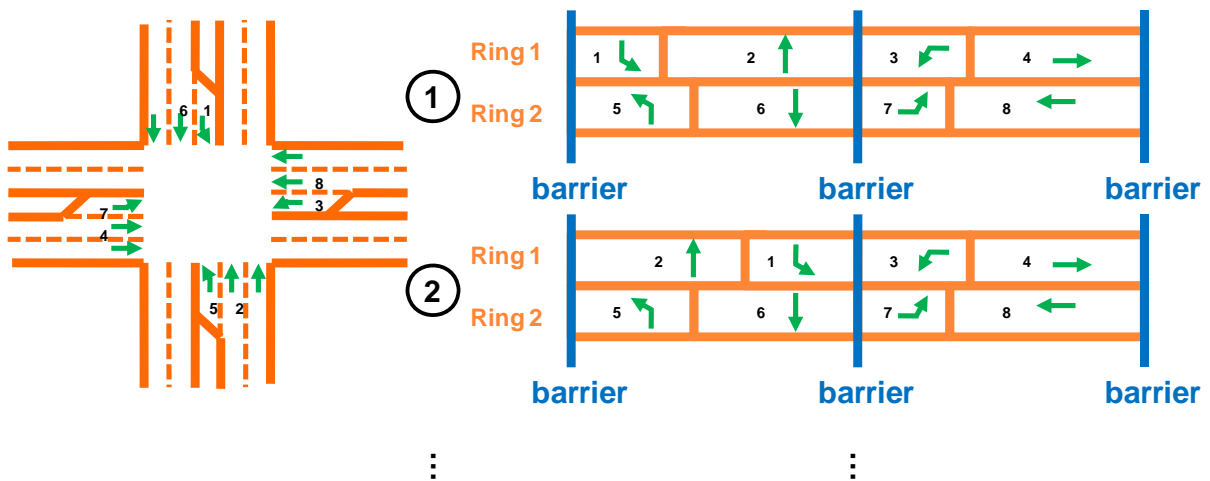
Figure 4-11 NEMA eight-phase signal timing structure

41

The following equations illustrate the two-ring eight-phase structure:

$$g_{k1} + g_{k2} = g_{k5} + g_{k6} \tag{4-22}$$

$$g_{k3} + g_{k4} = g_{k7} + g_{k8} \tag{4-23}$$

$$g_{k1} + g_{k2} + g_{k3} + g_{k4} = C_k \tag{4-24}$$

$$C_k = C/2^{h_k} \tag{4-25}$$

$$h_k = \begin{cases} 1, & \text{signal } k \text{ has half common cycle length} \\ 0, & \text{otherwise} \end{cases} \tag{4-26}$$

$$g_{kj} \geq MG_{kj}, j - 1, \dots, 8 \tag{4-27}$$

$$MinC \leq C_k \leq MaxC \tag{4-28}$$

$$0 \leq offset_k < C_k \tag{4-29}$$

$$g_{kj}, C_k, offset_k \text{ are integers} \tag{4-30}$$

Where, g_{kj} is the green time for Phase j of signal k, C_k is the cycle length of signal k; MGkj is the minimum green time of signal k at phase j; MinC is the minimum cycle length; MaxC is the maximum cycle length; C is the common signal cycle length; h_k is a binary variable that indicates whether signal k has a half common cycle length or not based the relation defined by Equation (4-26); and $offset_k$ represents the offset of signal k. Equations (4-22) and (4-23) indicate the existence of the signal barrier.

42

Equations (4-24) and (4-25) enforce the cycle length constraints. Equation (4-27) confines the green time of each phase to be less than its minimal green time; and Equation (4-28) specifies a user-defined minimal and maximal cycle lengths. Equation (4-29) requires that the offset of signal k lie between 0 and its cycle length.

To compute the green time for each interval t of the departure cell, it is essential to convert the green time of each phase as follows:

$$G_{k0} = G_{k4} = 0; \ G_{kt} = \sum_{j=0}^{t-1} g_{kj}, \ for \ t = 1,2,3 \tag{4-31}$$

$$G_{kt} = \sum_{j=4}^{t-1} g_{kj}, \ for \ t = 5,6,7 \tag{4-32}$$

Where G_{kt} is the total green time in the signal cycle illustrated in Figure 4-11.

4.3   Solution Algorithm

In the proposed model, the decision variables are the cycle length, green time split, and the offset of each signal. This study employs a Genetic-Algorithm-(GA)-based solution method for the proposed model. GA is a search technique that has been successfully applied to optimize signal timings under various traffic conditions (Daganzo 1995b). To speed up the computing process of convergence, this study applies the elitist selection method to optimize all decision variables (Ceylan 2006; Ceylan and Bell 2004; Lo and Chow 2004; Park et al. 1999; Zhou et al. 2007).

The most critical part of developing a GA-based algorithm is to derive a good encoding scheme, i.e., how to represent possible solutions of the target problem by a gene series of 0-1 bits. This study employs an encoding scheme which includes the constraints (4-22) to (4-30), i.e., the signal timing decoded from the scheme will be feasible to constraints (4-22) to (4-30). The fraction-based decoding scheme, based on the NEMA phase's structure proposed by Park, Messer et al. (1994) can satisfy all those constraints

except Equation (4-25). Hence, this study has grounded on their work, and extended its schema with the half common cycle length for certain signals.
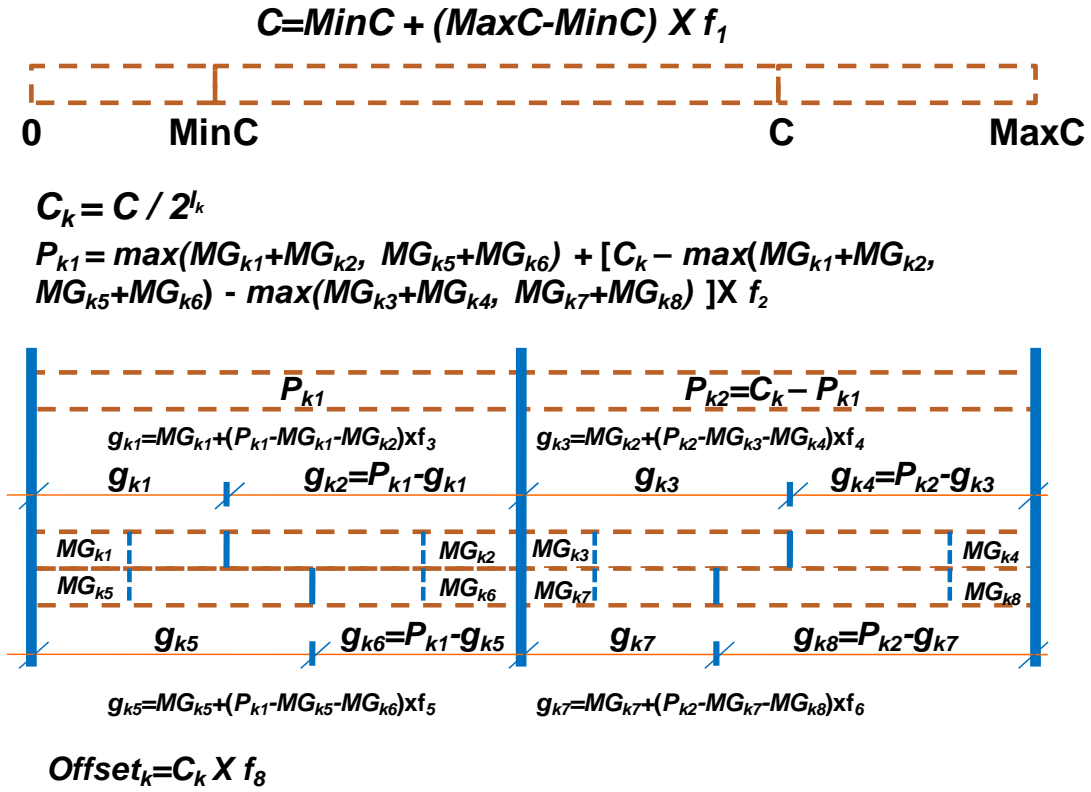
$$C = MinC + (MaxC - MinC) \times f_1$$

0 MinC   C   MaxC

$$C_k = C / 2^{l_k}$$

$$P_{k1} = max(MG_{k1}+MG_{k2},\ MG_{k5}+MG_{k6}) + [C_k - max(MG_{k1}+MG_{k2},$$
$$MG_{k5}+MG_{k6}) - max(MG_{k3}+MG_{k4},\ MG_{k7}+MG_{k8})\ ] \times f_2$$

P_{k1} $P_{k2}=C_k - P_{k1}$

$g_{k1}=MG_{k1}+(P_{k1}-MG_{k1}-MG_{k2})xf_3$ $g_{k3}=MG_{k2}+(P_{k2}-MG_{k3}-MG_{k4})xf_4$

g_{k1} $g_{k2}=P_{k1}-g_{k1}$ g_{k3} $g_{k4}=P_{k2}-g_{k3}$

MG_{k1} MG_{k2} MG_{k3} MG_{k4}

MG_{k5} MG_{k6} MG_{k7} MG_{k8}

g_{k5} $g_{k6}=P_{k1}-g_{k5}$ g_{k7} $g_{k8}=P_{k2}-g_{k7}$

$g_{k5}=MG_{k5}+(P_{k1}-MG_{k5}-MG_{k6})xf_5$ $g_{k7}=MG_{k7}+(P_{k2}-MG_{k7}-MG_{k8})xf_6$

$$Offset_k = C_k \times f_8$$

Figure 4-12 An enhanced fraction-based decoding scheme for signal design

A detailed description of the original scheme can be found in the literature. As illustrated in Figure 4-12, the proposed scheme sets the cycle length of signal k to half of a common cycle length if the half-cycle binary variable, I_k, is 1. Otherwise, the cycle length is set to be the full common cycle length.

4.4   Conclusions

This study has presented an enhanced Cell-Transmission Model for optimizing signal plans at intersections along a congested arterial. The proposed model with its innovative sub-cell modeling methodology is capable of capturing traffic flow interactions between neighboring lane groups due to queue spillback under high volume conditions. The arterial signal optimization model reported in the chapter can optimize

the cycle length, split, and offset, under the presence of the link and lane group blockages.

CHAPTER 5: AN INTEGRATED INTERCHANG CONTROL MODEL

5.1   Introduction

This chapter presents an integrated optimal control model that grounds on the arterial signal optimization model, but extends its formulations to capture the impact of off-ramp queue spillback to the freeway mainline at the interchange. The proposed interchange control model includes the freeway mainline traffic delays caused directly and indirectly by the moving queue at the off-ramp, and thus allows traffic engineers to assess the tradeoff between the freeway and its neighboring arterial congestion under various traffic conditions.

Figure 5-13 illustrates a signalized interchange, which includes two closely spaced signals and two on- and two off-ramps. The distance between these two signals typically ranges from 500 ft in urban areas to 800 ft in suburbs. The short distance between these two intersections for receiving freeway traffic offers a very limited queue storage capacity, and thus often causes queue spillback between them under oversaturated conditions. For instance, insufficient signal timing for the off-ramp at intersection-2 may cause its queue to spill back to the rightmost lane of the freeway mainline segment, and consequently increase its lane-changing density in the traffic flow. Conversely, inadequate green duration for the arterial through traffic could create a link blockage between two intersections. Thus, it is essential to have an integrated control system that can best allocate the signal timings for all control points under various congestion levels from the perspective of the system optimization.
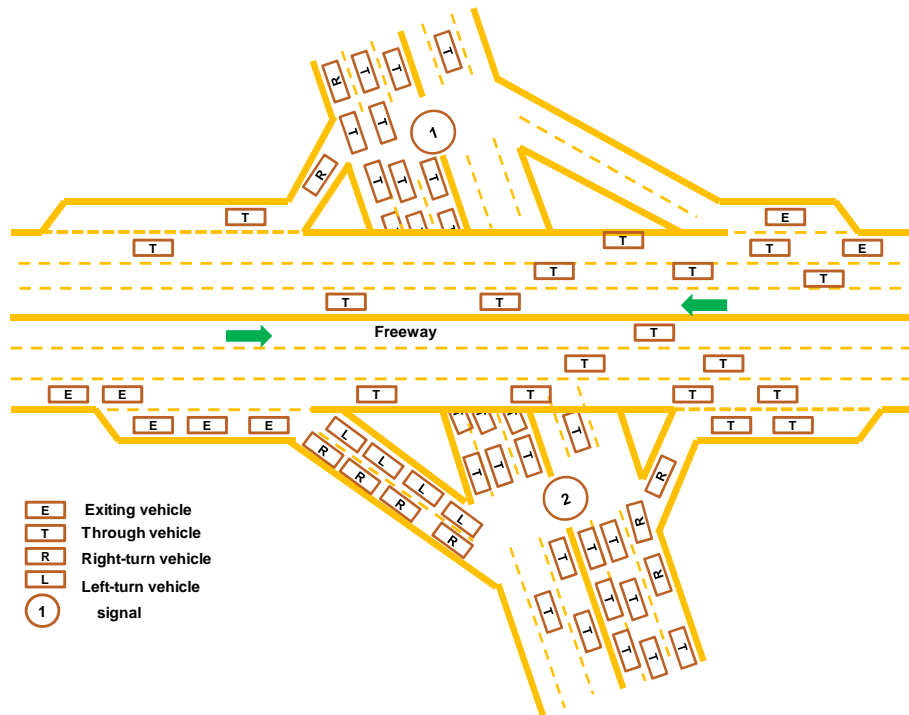
Figure 5-13 Graphical illustration of a signalized interchange

This chapter hereafter focuses on illustrating the formulation of a freeway model and its integration with the optimal arterial signal model presented in the previous chapter. The proposed freeway traffic model aims to capture the following two types of complex traffic flow interrelationships: (1) the impacts of arterial traffic volume on the off-ramp queue length; and (2) the spillback of ramp queue vehicles on the delay and operational capacity of its neighboring freeway travel lanes.

The remaining sections of this chapter are organized as follows. Section 5.2 presents the core logic of the proposed freeway traffic flow model. Section 5.3 illustrates the mathematical formulations for complex interactions between traffic flows and the model solution algorithm. Section 5.4 summarizes the concluding comments.

5.2   Modeling Methodology for Freeway

Figure 5-14 illustrates a typical freeway mainline segment that consists of two different segments, named Type-A and Type-B. Vehicles in the Type-A segment can head to either the downstream freeway mainline or the off-ramp, where all vehicles in the Type-B segment will move only to the downstream mainline segment.

To facilitate the formulations of the complex interactions between the freeway and ramp flows with the CTM methodology, this study first defines the following key parameters:

- Time t : the time interval $[t, t+1]$:

- n_i^t: the number of vehicles in Cell I;

- N_i^t: the buffer capacity, defined as the maximum number of vehicles that can be in Cell i at time t, which is the product of the cell length multiplied by the jam density;

- Q_i^t: the flow capacity in time t, and defined as the maximum number of vehicles that can move into Cell i;

- y_{ij}^t: the number of vehicles leaving cell i and entering cell j in time t.
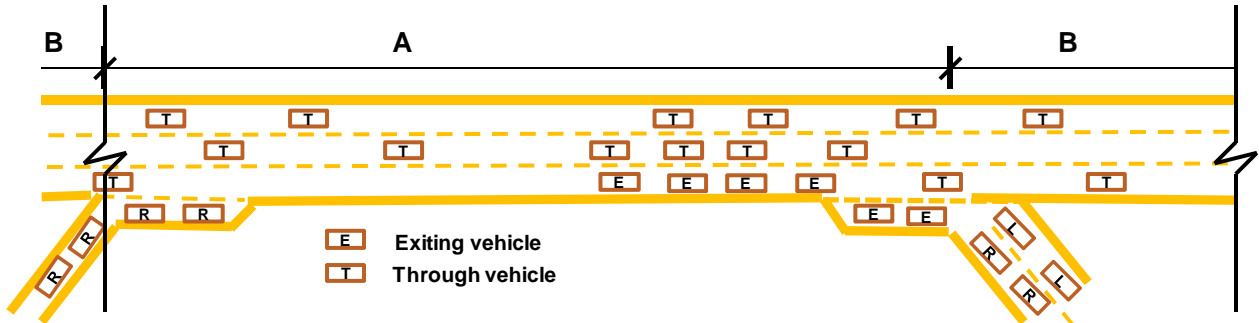
Figure 5-14 The freeway segments by destination

5.2.1 Modeling of Type-B Segments

Type-B segment contains one entry and one exit cells as shown in Figure 5-15. Equation (5-33) illustrates the relations for computing the number of vehicles that can exit from Cell i and enter Cell $i+1$ in time t, i.e., $y_{i,i+1}^t$.

$$y_{i,i+1}^t = \min\{n_i^t, Q_i^t, \delta[N_{i+1} - n_{i+1}^t]\} \tag{5-33}$$

Where $\delta = 1, if\ n_i^t \leq Q_i^t$, and $\delta = \frac{w}{v}, if\ n_i^t > Q_i^t$, in which w represents the disturbances

propagate backward speed, and v is the free-flow speed.

Let $S_i^t(= \min\{Q_i^t, n_i^t\})$ be the sending capacity, and $R_i^t = \min\{Q_i^t, \delta(N_i^t - n_i^t)\}$

as the receiving capacity of Cell t, then one can rewrite Equation (5-33) as follows:

$$y_{i,i+1}^t = \min\{S_i^t, R_{i+1}^t\} \tag{5-34}$$
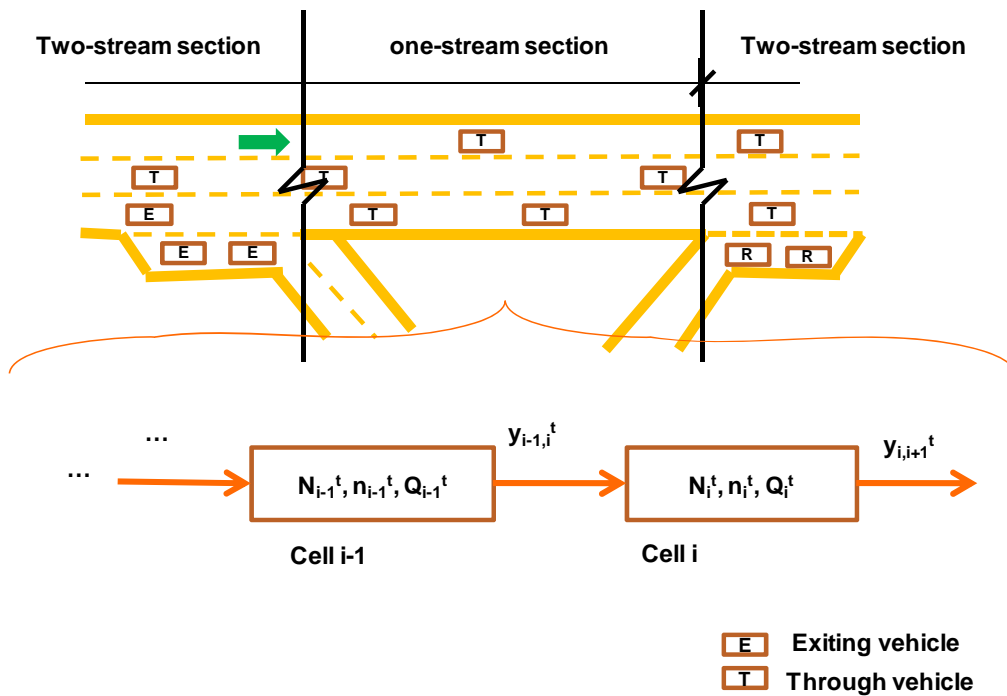
Figure 5-15 Modeling the traffic flow interactions in Type-B segment by CTM

Equation (5-35) represents the flow conservation relationship in the cell level, implying that the vehicle number of a cell in the next time interval equals the number of vehicles present in this interval and all entering vehicles but subtracting all leaving vehicles.

$$n_i^{t+1} = n_i^t + y_{i-1,i}^t - y_{i,i+1}^t$$

(5-35)

4.1.2 Modeling of Type-A Segments

To model Type-A freeway segment, it is necessary to add one additional state variable, $n_{E,i}^t$, and track the exiting number of vehicles with the following expression:

$$y_{E,i,i+1}^t = \min\{r_{E,i}^t \times \min\{n_i^t, Q_i^t, \delta(N_{i+1} - n_{i+1}^t)\}, N_{E,i+1}^t - n_{E,i+1}^t\}$$

(5-36)

Where $y_{E,i,i+1}^t$ denotes the exit number of vehicles from Cell i to Cell $i+1$; $r_{E,i}^t$ is the

exiting percentage of vehicles in Cell i for time interval t, which can be computed as

$r_{E,i}^t = n_{E,i}^t / n_i^t$; $N_{E,i+1}^t$ is the buffer capacity for exiting traffic, i.e., the maximum number

of exiting vehicles that can stay in cell i.
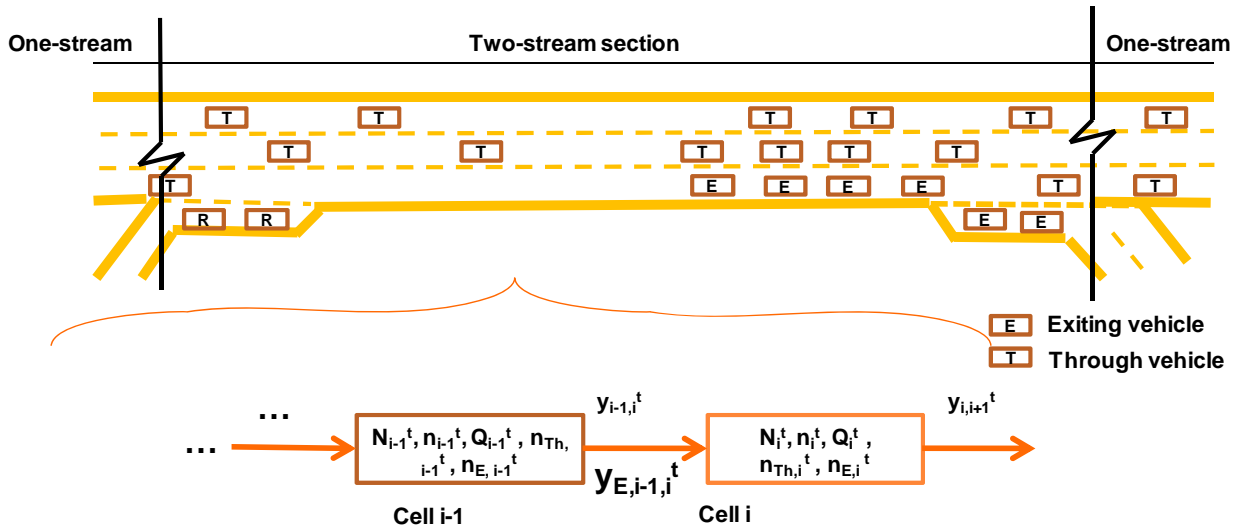
Figure 5-16 Modeling the one-stream segment by cell

$$y_{i,i+1}^{t} = \left(1 - \gamma_{E,i}^{t}\right) \times min\{n_i^t, Q_i^t, \delta[N_{i+1} - n_{i+1}^t]\} + y_{E,i,i+1}^{t}$$ (5-37)

Equation (5-37) determines the total vehicle number from Cell i+1 to its downstream cell (Cell i). The underlying assumption is that the two different traffic streams are well mixed.

$$n_{E,i}^{t+1} = n_{E,i}^t + y_{E,i-1,i}^t - y_{E,i,i+1}^t$$ (5-38)

Equation (5-35) illustrates the flow conservation relationship within each two-stream cell. In addition, Equation (5-38) also represents the conservation law of the exiting flows if without queue.
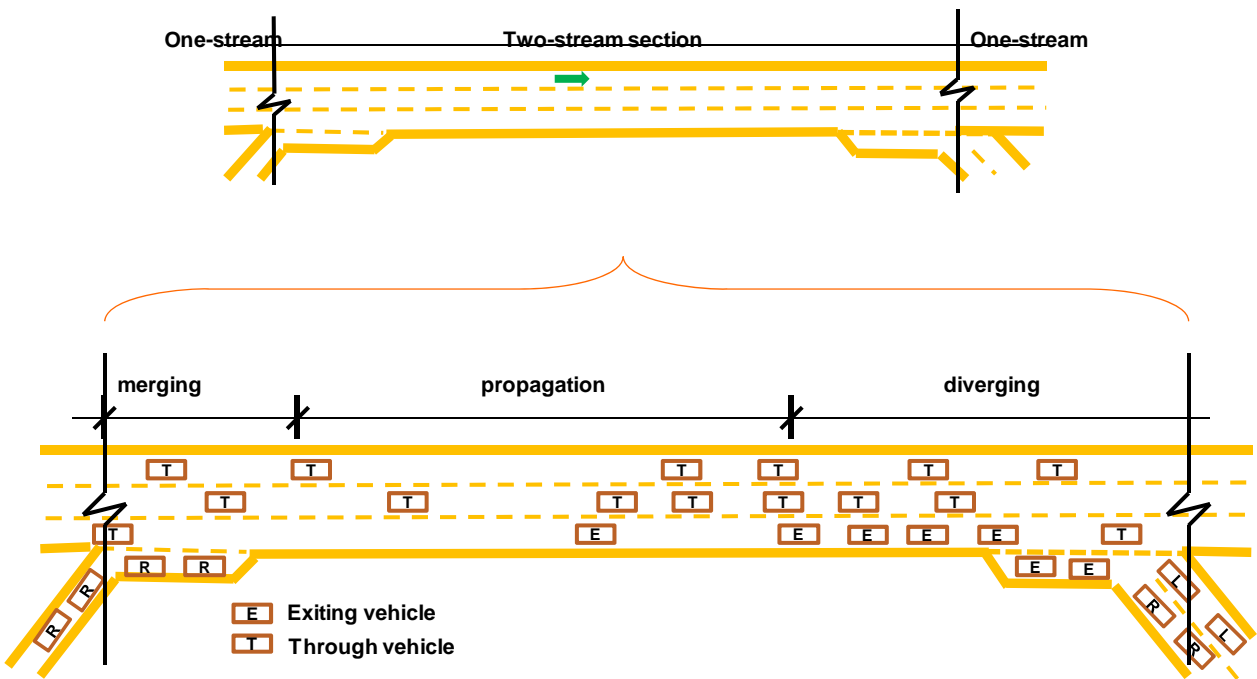
Figure 5-17 Type-A segment traffic dynamics

As shown in Figure 5-17, one can further divide the Type-A segment into merging zone, propagation zone and diverging zone. Among these three zones, the propagation zone can be represented with the ordinary two-stream cells to capture the

traffic dynamics. The modeling methodologies for merging zone and diverging zone are presented below.

Merging zone

As illustrated in Figure 5-18, one can use a merging cell (Cell C) to represent the merging zone, which consists of one entry cell for the upstream freeway segment and the other for the on-ramp. As the on-ramp traffic should yield to the freeway mainline flow, it is natural to determine the mainline entry volume (y_{BC}^t) first, and then the on-ramp entry volume after updating the merging cell vehicle number n_C^t by adding the entry vehicle number from the upstream freeway mainline cell (y_{AC}^t). Therefore, one can use Equations (5-39) and (5-40) to determine the entry flow from upstream freeway mainline and on-ramp.

$$y_{AC}^t = \min\{n_A^t, Q_A^t, \delta[N_C - n_C^t]\} \tag{5-39}$$

$$y_{BC}^t = \min\{n_B^t, Q_B^t, \delta[N_C - n_C^t - y_{AC}^t]\} \tag{5-40}$$

$$y_{E,iC}^t = y_{iC}^t \times \zeta_{E}^t, i = A, B \tag{5-41}$$

Where ζ_E^t is the predetermined exiting volume percentage of the downstream freeways segment at time interval *t*.
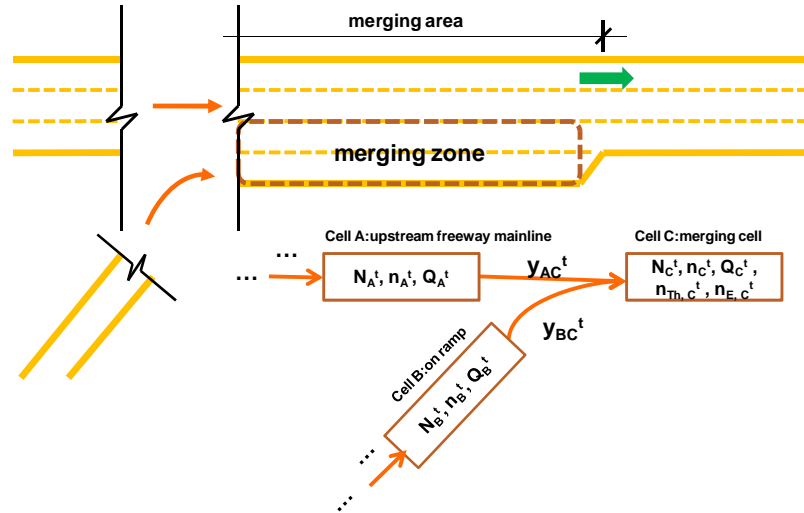
Figure 5-18 On-ramp traffic characteristics

The entry capacity of on-ramp, Q_B^t, is determined by the traffic dynamics in the merging zone as shown in Figure 5-18. The length of the acceleration lane and the traffic stream characteristic in the adjacent freeway lane are the two primary factors that may affect Q_B^t. In this study, Q_B^t is determined with Equation (5-42).

$$Q_B^t = (Q_A^t - y_{AC}^t) \times p_C^t \qquad (5\text{-}42)$$

Where p_C^t is the vehicle proportion which is on the right-most lane at time interval t.

Equation (5-42) assumes that the on-ramp traffic could take all the remaining capacity of the right-most freeway lane.

Diverging zone

Under congested conditions, it is quite often that the off-ramp queue could spill back to the upstream freeway mainline, and occupy one or two through lanes. Also, the speed of the neighboring mainline lanes may also be reduced due to a high frequency of lane changing maneuvers.
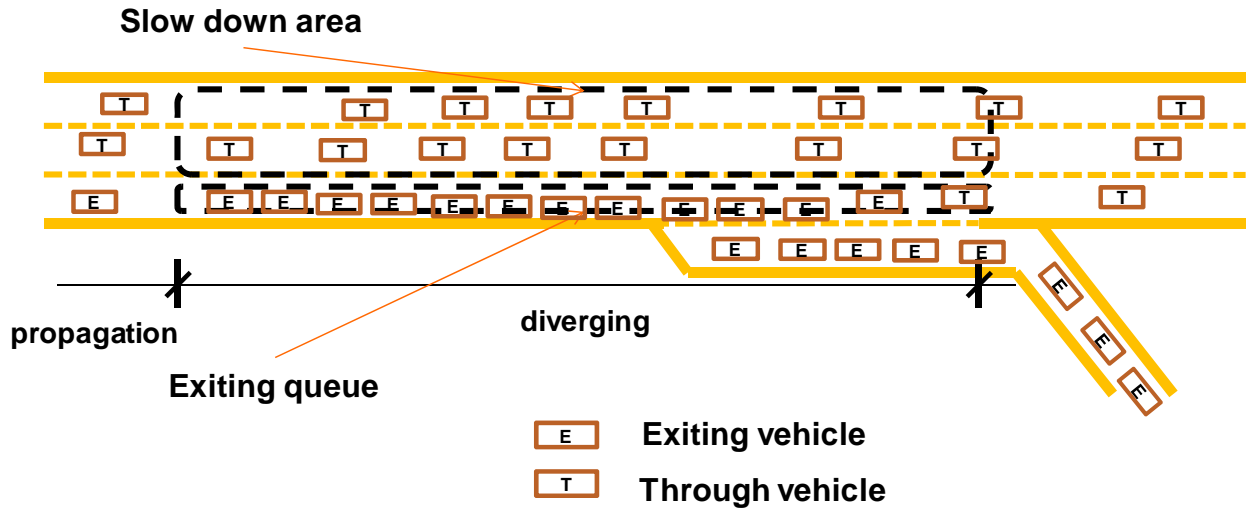
Figure 5-19 Exiting-queue effect in a diverging zone

To reflect the impact of such complex flow interactions on the freeway mainline capacity, one can model the diverging zone with a diverging cell (named Cell A) and let its two downstream cells (Cell B and Cell C) represent the downstream off-ramp and freeway mainline segment, respectively (see Figure 5-20). The diverging zone under the proposed methodology shall consist of three sub-areas, denoted as TH, TE, and E. In sub-zone TH, all vehicles will head to the downstream mainline, whereas vehicles in sub-zone E will exit mainly to the adjacent off-ramp. In contrast, both through and existing vehicles can share the space in sub-zone TE.

Figure 5-8 illustrates the concept of modeling each diverging cell with two sub-cells (Sub-cell TH and Sub-cell E) to represent its two different outgoing traffic streams. One can thus approximate the buffer capacity of Sub-cell TH, denoted as N_{Th}^i, with the equation $N_{Th}^i = N_1^i + N_2^i$. Likewise, the buffer capacity of Sub-cell E, N_E^i, is equal to the sum of $N_2^i + N_3^i$, where N_1, N_2 and N_3 are the maximum number of vehicles that can stay in each sub-zone.
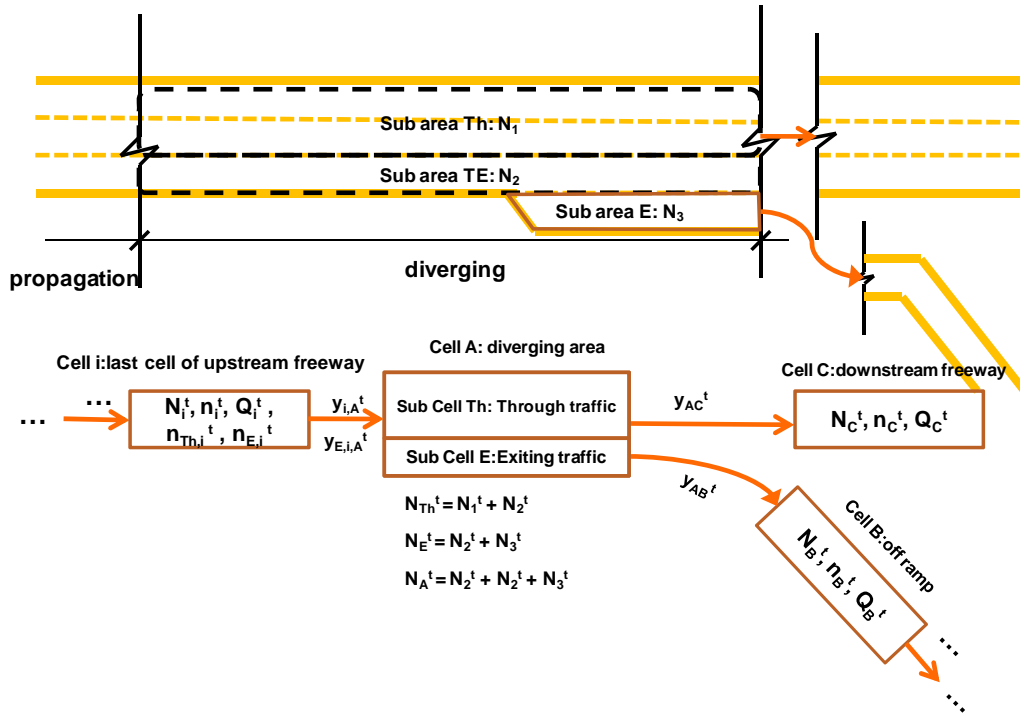
Figure 5-20 Graphical illustration of the modeling concept for the diverging zone

$$y = min\{n_i^E, Q_i^E, \delta(N_A^E - n_A^E)\} \tag{5-43}$$

$$y_{E,i,A}^t = min\{y\gamma_{E,i}^t, N_{E,A}^t - n_{E,A}^t\} \tag{5-44}$$

$$y_{i,Th}^t = min\{(1-\gamma_{E,i}^t) \times y, N_{Th}^t - n_{Th}^t\} \tag{5-45}$$

$$y_{iA}^t = y_{i,Th}^t + y_{E,i,A}^t \tag{5-46}$$

Where y is a temporary variable to simplify description; $y_{i,Th}^t$ stands for the vehicle

number from cell i to the Sub-cell TH of cell A; $y_{E,i,Th}^t$ denotes those vehicles which miss

the off-ramp due to spillback. Equations (5-44) and (5-45) determine the total vehicle number from Cell i to the through sub cell of the diverging cell (Sub-cell TH of Cell A) and the exit sub cell (Sub-cell E of Cell A), which assumes that the two different traffic streams are well mixed. The exiting flows from the sub cells to its downstream cell follow Equations (5-47) and (5-48). Note that all those cells or sub-cells share the identical flow conservation relationships.

$$y_{Ac}^t = min\{n_{Th}^t, Q_{Th}^t, \delta(N_C^t - n_C^t)\}$$

(5-47)

(5-48)

$$y_{AB}^t = min\{n_E^t, Q_E^t, \delta(N_B^t - n_B^t)\}$$

The saturated flow rate of the exiting sub-cell (sub-cell E) is clearly equal to the off-ramp saturated flow rate. However, computing the saturated flow rate for the through sub-cell (Sub-cell TH) is relatively complex. As mentioned previously, when the exiting queue from an off-ramp spills back to the freeway mainline, some length of mainline lanes neighboring to the off-ramp will become a slow-speed zone due to the rubbernecking and lane-changing effects. Equation 5-17 illustrates such an impact and the interrelationships between all contributing variables:

$$Q_{Th}^t = Q_A \times \left(1 - \frac{L_{A,E}}{L_A}\right) \times [1 - \alpha_A \times \frac{n_{E,A}^t}{N_{E,A}^t}]$$

(5-49)

Where $L_{A,E}$ is the number of lane occupied by the exiting queue; L_A is total lane number of the freeway mainline; $Q_A \times (1 - L_{A,E}/L_A)$ is the capacity of the unblocked through lane(s); α_A is the maximal saturated flow deduction proportion, which is the reduced percentage of capacity when the exiting vehicles occupy all available buffer space of the

freeway; $n_{E,d}^t/N_{E,d}^t$ is the proportion of the exiting buffer capacity occupied by the

exiting vehicles. Equation (5-49) assumes that the through saturated flow rate equals the capacity of remaining though lane(s) subjected to a reduction factor that increases with the exit queue length.

5.3 An integrated single-interchange control model

Objective function

Depending on the traffic conditions, one can set the control objective to maximize the total system throughput or minimize the total delay. With the above cell-based formulations, the objective function of maximizing the system throughput can be expressed as follows:

$$Max \ (Throughput = \sum_{t=1}^{T}\sum_{j\in S}\sum_{i\in\Gamma^{-}(j)} y_{ij}^t) \tag{5-50}$$

Where S is the sink cell set, $\Gamma^{-}(j)$ is the upstream cell set of cell j, and T is total operating time period.

As mentioned in Chapter 4, the length of each cell is set to be the free-flow travel distance during a pre-specified time unit, which implies that vehicles in each cell can either stay or move to the downstream cells during each time interval. Hence, one can approximate the delay as the difference between a vehicle's actual travel time and its free-flow travel time over a given travel distance. For instance, if some vehicles staying in the same cell over n consecutive unit intervals, then it implies that they all have experienced the delay of n unit times. More specifically, one can define the delay for each cell for time interval t as $d_i^t = \left(n_i^{t-1} - \sum_{j\in\Gamma(i)} y_{ij}^t\right)\tau$, where $\Gamma(i)$ is the downstream cell set of Cell i and τ is the length of one time unit. The alternative objective function of minimizing the total system delay can be expressed as follows:

$$Min \left[total\ delay = \tau \sum_{t=1}^{T} \sum_{i} \sum_{j \in \Gamma(i)} (n_i^t - x_{ij}^t) \right]$$ (5-51)

As τ is a constant, the minimal system delay objective function can further be stated as:

$$Min\ z = \sum_{t=1}^{T} \sum_{i} \sum_{j \in \Gamma(i)} (n_i^t - x_{ij}^t)$$ (5-52)

The formulations for signal control and the solution algorithm are identical to those presented in Chapter 4, except the inclusion of freeway related constraints.

5.4   Conclusion

This chapter presents an interchange integrated control with the Cell-Transmission concept. The proposed formulations reflect the complex interactions between ramp queue and mainline vehicles in the merging, propagation, and diverging zones at a typical freeway interchange. By integrating the arterial signal models with the freeway formulations, one can operate the ramp and signal control plan from the perspective of optimizing the efficiency of the entire interchange, including the tradeoff between freeway and arterial delays.   Due to the embedded relations for capturing the queue spillback impacts on neighboring traffic flow movements, the proposed interchange model is able to generate the optimal control strategies for oversaturated traffic conditions during congested peak commuting hours.

CHAPTER 6: EXPERIMENTAL ANALYSES

6.1 Introduction

This chapter presents the experimental results with the proposed arterial and off-ramp control models using field data from a congested interchange on the I-495 Capital Beltway. The performance evaluation first focuses on the delay and throughput of the entire arterial within the control boundaries, and then compares the tradeoff between freeway and arterial delays that take into account the ramp queue impacts on the freeway mainline traffic. To assess the effectiveness of our proposed models, this chapter also presents their comparison results with TRANSYT-7F, one of the state-of-the-art software for arterial signal optimization.

The remaining sections of this chapter is organized as follows: Section 6.2 describes the target interchange on the I-495 Capital Beltway for experimental design, including its geometric features, traffic demand patterns, and selected measures of effective (MOE) for performance comparison. Section 6.3 reports the evaluation results for the arterial signal optimization model and its comparison with the performance of TRANSYT-7F. Section 6.4 analyzes the effectiveness of the proposed interchange control model for concurrent minimization of delay on both the freeway and local intersections within the control boundaries.

6.2 Experimental Design

Figure 0-21 shows the network configuration of the interchange between the Capital Beltway (I-495) and Georgia Avenue (MD97), including four signalized intersections from Forest Glen Rd (MD192) to Seminary PI, and four major congested highway segments: I-495 Outer Loop (I-495 OL), I-495 Inner Loop (I-495 IL), MD 97 Southbound (MD 97 SB), and MD 97 Northbound (MD97 NB).
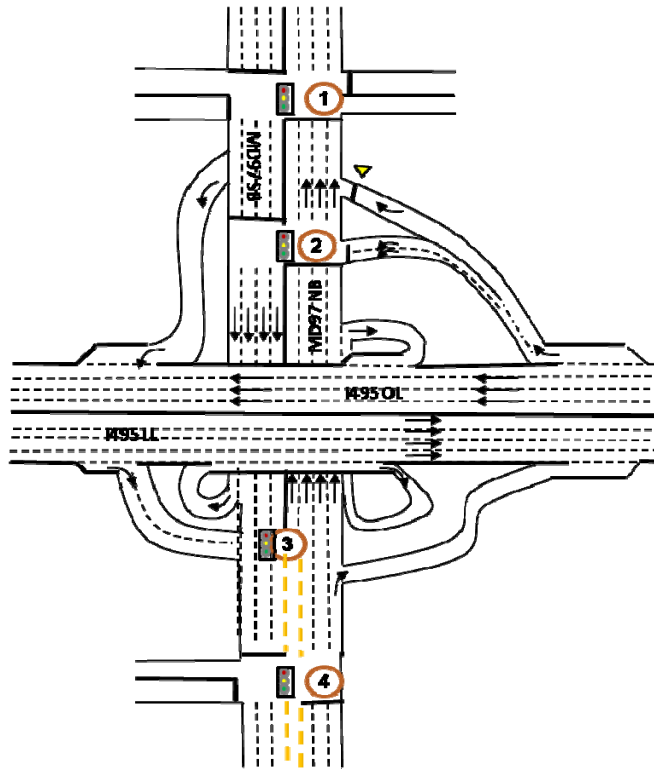
Figure 0-21 Graphical illustration of the target interchange

Parameters for the solution algorithms

      All experimental scenarios in Table 6-1 employ the specially-designed GA algorithm to compute the parameters for the optimal system-wide control. Each experimental scenario also applies TRANSYT-7F (Release 10), one of the most advanced signal optimization programs for both research and practice, to generate the alternate set of control parameters. To be on the same basis for comparison, this study selects the same GA algorithm embedded in TRANSYT-7F to all experimental scenarios, and also uses the same set of parameters such as 200 generations with a population size of 50, the crossover probability of 0.3, and a mutation probability of 0.01.   The corridor simulation program, CORSIM, generally used by the research community is the tool for use to simulate all traffic scenarios listed in each experiment, and generate their MOEs under the optimal control strategies produced by TRANSYT-7F and the proposed model.

6.3 Experimental Results of the Arterial Signal Optimization Model

Control boundaries

Figure 6-2 illustrates the control boundaries in each experimental scenario, which includes four intersection signals and two arterial segments of MD97SB and MD97NB.
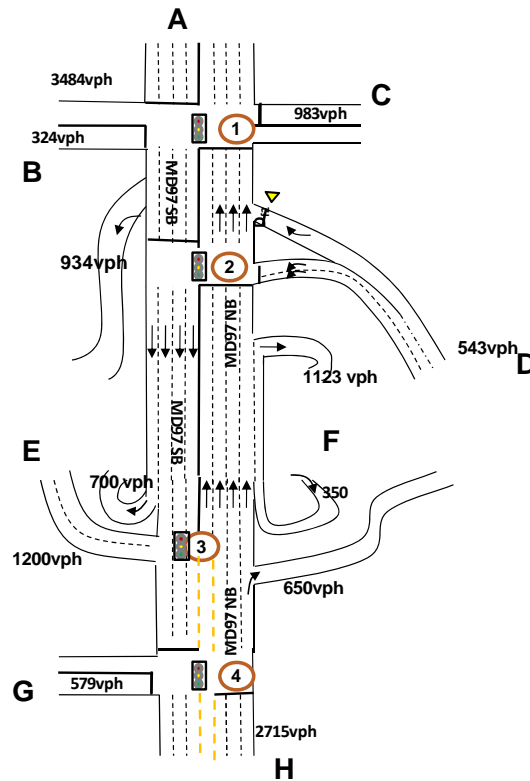
Figure 0-22 Control boundaries of the case study for arterial signal optimization

Traffic demand patterns

Table 6-1 summarizes the distribution of volume data for performing the numerical experiments and analyses, based on the day–to-day variation of field data from each entry and exiting control points within the control boundaries. Note that the volume used in the experimental scenarios is increased at the rate of 10 percent from the low, medium, and to the high levels, based on the field data. Figure 6-2 shows each key location within the control boundaries.

Table 0-1: Demand scenarios for arterial signal optimization model (vehicle per hour)

Entrance	Movements	Demand Scenario		

		Low	Medium	High
A	Through	3,044	3,382	3,720
	Right	101	112	123
B	Left	40	44	48
	Through	91	101	111
	Right	161	179	197
C	Left	536	596	656
	Through	306	340	374
	Right	42	47	52
D	Left	284	315	347
	Right	204	227	250
E	Right	1,080	1,200	1,320
F	Right	315	350	385
G	Left	498	553	608
	Right	23	25	28
H	Through	2,444	2,715	2,987
Total	-----	9,167	10,186	11,204

Overall system performance comparison

Table 6-2 summarizes the MOEs of each experimental scenario under two
candidate control strategies for the low, medium, and high demand scenarios defined in
Table 6-1. All MOES were the average of 50 simulation runs over the duration of one
hour with CORSIM. The selected MOEs from simulation output include: network-wide
total delay and system throughput. The results presented in Table 0-2 indicate that the
proposed arterial optimization model outperforms TRANSYT-7F under all scenarios at
the system level.

Table 0-2: Overall model performance comparison

Demand Scenarios		Simulation Results from CORSIM (One hour)				
		The Proposed Model	TRANSYT-7F	Improvement*	Improvement * (%)	Improvement (95% CI*)
Low	Total Delay (vehicle-hour)	122.34	178.50	56.16	31%	[28.8,83.5]
	Total Throughput (vehicle)	9107.36	8990.10	117.26	1%	[54.5, 180.0]
Medium	Total Delay (vehicle-hour)	174.20	276.01	101.81	37%	[68.6,135.1]
	Total Throughput (vehicle)	10047.50	9870.52	176.98	2%	[78.1, 275.8]
High	Total Delay (vehicle-hour)	259.11	426.14	167.03	39%	[135.7,198.3]
	Total Throughput (vehicle)	10846.28	10192.18	654.10	6%	[567.7, 740.5]

* Delay improvement = TRANSYT-7F Delay – The Proposed Model Delay
Throughput improvement = The Proposed Model Throughput - TRANSYT-7F Throughput

Delay Improvement (%) = (TRANSYT-7F Delay – The Proposed Model Delay) / the Proposed Model Delay $\times 100\%$

Throughput Improvement (%) = (The Proposed Model Throughput - TRANSYT-7F Throughput) / TRANSYT-7F Throughput $\times 100\%$

C.I. = confidence Interval

For example, at the high congestion level, the target set of arterial intersections with the proposed signal model yields the total delay of 259 vehicle-hours, about 39 percent less than if using TRANSYT-7F. The same range of improvement also exists at the low and medium volume levels as shown in Table 6-2. The 95% confidence intervals for each scenario also confirm that the improvements are statistically significant, and increase with the congestion level or the total volume entering the control boundaries. The overall results seem to imply that the proposed arterial model with its explicit consideration of queue spillback and lane-blockage due to overflow is especially applicable for optimizing signals under congested conditions.

Delay comparison between intersections

Table 6-3 presents the delay incurred at those four intersections on MD 97 within the control boundaries. Based on the improvement by intersection, it is clear that the proposed control model, in comparison with TRANSYT-7F, can better redistribute the delays among all intersections, and significantly reduce the queue at the most congested one at the modest cost of other less congested intersections when the entire traffic system experiences a relatively low demand level. The similar redistribution patterns also exist among all intersections at the medium and high demand levels. As discussed previously, this is due likely to the fact that the proposed signal model takes into account the possible queue spillback at all congested intersection approaches, and offers sufficient signal timings to accommodate such flow patterns that in turn prevent the queue formation and propagation to its upstream links.

At the arterial level, the proposed signal control model yields a significantly lower total delay than TRANSYT-7F for MD 97 southbound (SB), a highly congested segment.

The performance of these two models for MD97 Northbound, however, are comparable because its volume is relative low, and not to cause any lane blockage or queue spillback.

In summary, the proposed arterial signal optimization model clearly outperforms the state-of-art program, TRANSYT-7F, at all different demand levels for the congested I-495/George Avenue interchange, regardless of the total delay or system throughput. The mechanism embedded in the proposed model to capture the delay caused by blockage between lanes and queue spillback has proved its effectiveness in redistributing the delays from the most congested one to the remaining intersections, thereby minimizing the likelihood of having local bottlenecks at all demand levels

Table 0-3: Total delay comparison by intersection (vehicle minutes)

Demand Scenarios		Simulation Results from CORSIM (One hour)				
		The Proposed Model	TRANSYT -7F	Improvement *	Improvement * (%)	Improvement (95% confidence interval)
Low	Intersection 1	2242.41	6112.78	3870.37	63%	[5483.4, 2257.4]
	Intersection 2	588.20	443.24	-144.95	-33%	[-109.1, -180.8]
	Intersection 3	1815.50	1703.63	-111.87	-7%	[-32.1, -191.7]
	Intersection 4	1235.07	1064.19	-170.88	-16%	[-67.5, -274.2]
	MD 97 SB	3951.1	7207.9	3256.8	45%	[1668.9, 4844.7]
	MD 97 NB	1475.1	1637.7	162.6	10%	[101.4, 223.7]
Medium	Intersection 1	3771.26	9376.52	5605.26	60%	[7742.7, 3467.9]
	Intersection 2	537.45	640.41	102.97	16%	[161.3, 44.6]
	Intersection 3	1992.82	2183.95	191.13	9%	[277.0, 105.2]
	Intersection 4	2318.74	1960.66	-358.09	-18%	[-221.3, -494.8]
	MD 97 SB	4261.0	11943.5	7682.5	64%	[5843.2, 9521.8]
	MD 97 NB	2011.0	2010.3	-0.7	-0%	[-84.7, 83.3]
High	Intersection 1	5967.06	16664.37	10697.31	64%	[12008.3, 9386.3]
	Intersection 2	964.92	895.53	-69.39	-8%	[284.9, -423.7]
	Intersection 3	2992.88	2779.33	-213.55	-8%	[57.8, -484.9]
	Intersection 4	2689.92	2590.17	-99.75	-4%	[-8.0, -191.5]
	MD 97 SB	6671.8	17109.8	10438.0	61%	[8845.1, 12031.0]
	MD 97 NB	2854.6	2961.3	106.7	4%	[-73.4, 286.9]

Delay Improvement (%) = (TRANSYT-7F Delay – The Proposed Model Delay) / the Proposed Model Delay × 100%

C.I. = confidence Interval

6.4   Results of the Integrated Interchange Control Model

Control boundaries

Figure 6-3 illustrates the boundaries of the integrated interchange control model, including four arterial signals and two freeway segments (i.e., I-495WB and I-495EB).
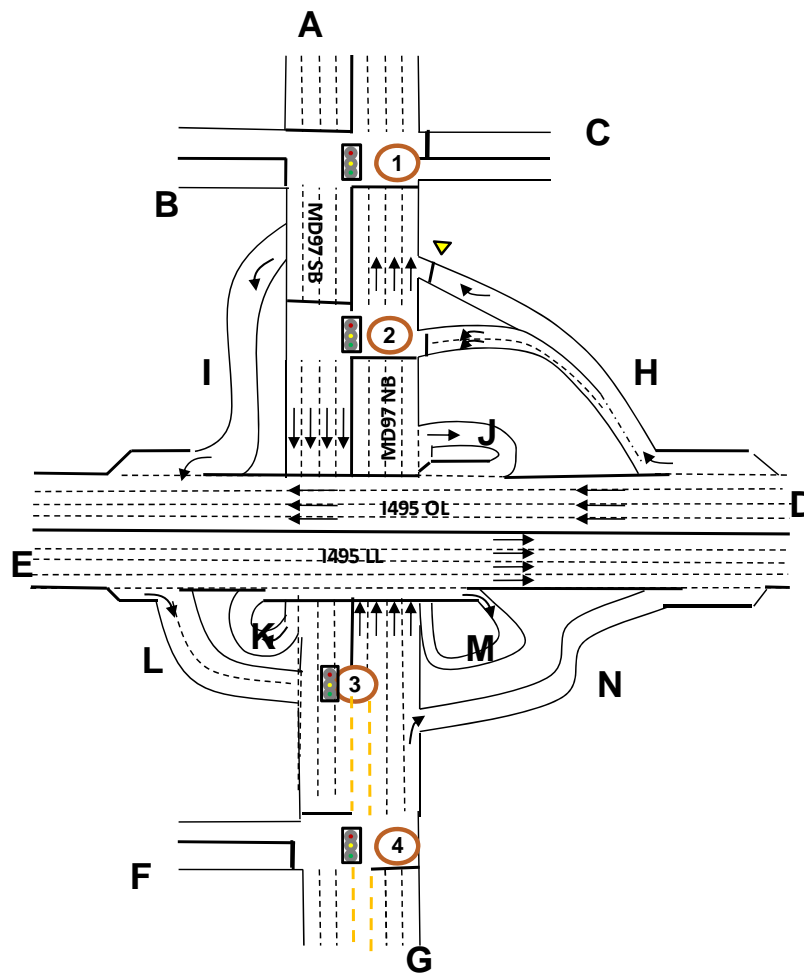

Figure 0-23 A graphical illustration of the example interchange

Traffic demand patterns

Table 6-4 presents the volume for each control points based on the field data, and Table 6-5 defines the demand from Ramp-H for analyzing of its impact on the overall system performance.

Table 0-4 Basic demand for entrances and ramps (vehicle per hour)

Entrance	Movements	Demand	Ramp	Movements	Demand
A	Through	3,382		Right	670
A	Right	112	H	Left	930
B	Left	44		Total	1600
B	Through	101	I	Enter	825
B	Right	179	J	Enter	1402
C	Left	596	K	Enter	829
C	Through	340	L	Exit	1179
C	Right	47	M	Exit	299
D	Through	7025	N	Enter	654
E	Through	6879			
F	Left	553			
F	Right	25			
G	Through	2,715			
Total	-----	21998			

Table 0-5 Exit volume scenarios' definition (vehicle per hour)

Entrance		Movements	Exit Volume Scenario (H Ramp)		
			Low	Medium	High
Ramp	H	Right	586	670	754
		Left	814	930	1046
		Total	1400	1600	1800

Table 0-6 Overall model performance comparison

Demand Scenarios	MOEs	Simulation Results from CORSIM (One hour)				
		ICIC*	TY7F*	Improvement*	Improvement * (%)	Improvement (95% CI*)
Low	Total Delay (vehicle-hour)	545.6	617.1	71.4	12%	[33.2, 109.6]
	Total Throughput (vehicle)	20591	20473	117	1%	[-67, 302]
Medium	Total Delay (vehicle-hour)	542.8	931.5	388.7	42%	[336.3, 441.0]
	Total Throughput	20735	18098	2637	15%	[2295, 2979]

High	(vehicle)					
	Total Delay (vehicle-hour)	455.9	943.2	487.3	52%	[402.4, 572.2]
	Total Throughput (vehicle)	20887	19057	1831	10%	[1241, 2421]

* ICIC: the proposed Interchange Integrated Control Model

TY7F: TRANSYT-7F

Delay improvement = TRANSYT-7F Delay – The Proposed Model Delay

Throughput improvement = The Proposed Model Throughput - TRANSYT-7F Throughput

Delay Improvement (%) = (TRANSYT-7F Delay – The Proposed Model Delay) / the Proposed Model Delay $\times 100\%$

Overall system performance comparison

Table 6-6 presents the network-wide total delay over one hour produced from the simulation program, CORSIM, under the control strategies by the proposed interchange model and TRANSYT-7F. As expected, the proposed interchange model outperforms TRANSYT-7F regarding the total delay at all three volume levels. The computed 95% confidence intervals also confirm that the improvements are statistically significant, and increase with the congestion level.

With respect to throughput, the proposed model yields a comparable level of performance with TRANSYT-7F under the low volume scenario. This is understandable because the system throughput generally equals its total demand if without congestion, regardless of the implemented control strategies. However, as the volume increases and congestion may occur, then whether an implemented control model is effective or not will impact significantly on the resulting throughput. This is evidenced by the better performance of the proposed model in comparison with TRANSYT-7F at the moderate and high demand levels.

Delay comparison between all control locations

Note that the total system delay under the control strategies by the proposed interchange model actually decreases with an increase in the Ramp-H volume. Table 0-7 presents the total delays on both the freeway and arterial segments within the control boundaries under three different volume levels. The results indicate that the proposed model yields the comparable level of freeway delay (16312 vs. 16091 veh-minutes) but

far less arterials delay (16426 vs. 20931 veh-minutes) than with TRANSYT-7F under the low demand level.

The improvements become much more pronounced if the traffic volume exiting from off-ramp-H increases from the medium to a high congested level. For instance, the total freeway delay reduces from the medium level of 14,350 veh-minutes to the high level of 12,459 veh-minutes under the proposed model, compared to 15,997 veh-minutes and 20,552 veh-minutes if with TRANSYT-7F. These results seem to reflect first the need to consider the impact of queue spillback on the freeway delay in design of the interchange control strategies, and secondly the potential of the proposed model that clearly outperforms TRANSYT-7F, one of the most powerful program for arterial signal design but not including the off-ramp queue impact on the freeway.

Table 0-7 Total delay comparison by roadway segment (vehicle minutes)

Demand Scenarios			Simulation Results from CORSIM (One hour)				
			ICIC	TY7F	Improvement*	Improvement * (%)	Improvement (95% confidence interval)
Low	Freeway	I495IL	5219.0	5124.3	-94.7	-1.8%	[-981.2, 791.9]
		I495OL	10807.5	10654.7	-152.8	-1.4%	[-1288.5, 982.9]
		Total	16312.2	16091.9	-220.3	-1.4%	[-1619.7, 1179.0]
	Arterial	MD97NB	2795.9	2866.2	70.4	2.5%	[-74.6, 215.3]
		MD97SB	7439.4	14811.7	7372.2	49.8%	[5738.9, 9005.6]
		Total	16426.4	20931.6	4505.3	21.5%	[2572.7, 6437.9]
Medium	Freeway	I495IL	5253.9	4390.0	-863.9	-19.7%	[-1276.5, -451.2]
		I495OL	8785.4	11195.1	2409.7	21.5%	[-90.7, 4910.1]
		Total	14350.2	15997.9	1647.7	10.3%	[-897.2, 4192.6]
	Arterial	MD97NB	3128.8	4186.6	1057.8	25.3%	[885.2, 1230.4]
		MD97SB	9176.8	29802.4	20625.5	69.2%	[17740.5, 23510.5]
		Total	18220.1	39892.8	21672.7	54.3%	[18629.4, 24716.0]
Hig	Fre	I495IL	5333.8	10220.3	4886.4	47.8%	[2617.3, 7155.6]

69

	I495OL	6787.1	9665.4	2878.3	29.8%	[585.6, 5170.9]
	Total	12459.7	20552.8	8093.1	39.4%	[4745.9, 11440.3]
Arterial	MD97NB	2558.9	5520.5	2961.6	53.6%	[2800.2, 3123.0]
	MD97SB	6650.7	22999.8	16349.2	71.1%	[13380.5, 19317.8]
	Total	14894.9	36041.1	21146.2	58.7%	[18071.6, 24220.7]

* Delay improvement = TRANSYT-7F Delay – The Proposed Model Delay

Delay Improvement (%) = (TRANSYT-7F Delay – The Proposed Model Delay) / the Proposed Model Delay $\times$ 100%

C.I. = confidence Interval

Freeway total delay comparison

Figure 0-24 and Figure 0-25 illustrates the relationship between the delay and the volume exiting from off-ramp H. Results from both figures and Table 6-7 indicate that the delay on I-495 IL is relatively stable as its traffic conditions are less likely to be impacted by the volume change at Ramp-H. On contrast, the total delay incurred on I-495 OL at the same total system demand level expectedly decreases with an increase in the off-ramp H volume, since the arterial signals have taken the freeway delay into account in computing the green times for the increased flows, and the freeway segment experiences a reduced volume on the mainline but no impact by the off-ramp queue. This explains why the I-495 OL delays under TRANSYT-7F are about 20 to 30 percent higher than the proposed model.
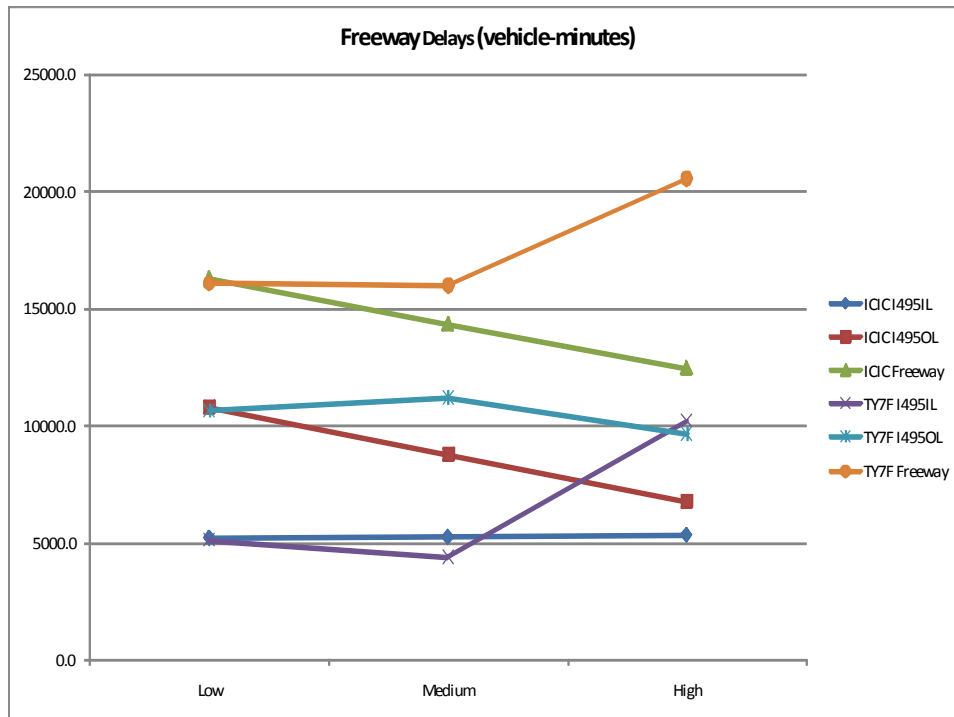
Figure 0-24 Comparison freeway delay by segment

Arterial delays comparison

Considering the arterial delays illustrated in Figure 0-25, the proposed integrated control model clearly outperforms TRNASYT-7F under the same local traffic demand but different off-ramp volumes. For instance, the total arterial delay under the proposed model during the medium off-ramp-H volume was 18220.1 vehicle-minutes, far less than the total of 21672 vehicle minutes if with the TRANSYT-7F model. The proposed integrated model also demonstrates the same superior performance under the scenario of having a high Ramp-H volume (i.e., 14894 vehicle-minutes versus 21146 vehicle-minutes).

Note that the proposed integrated control model with its embedded formulations for queue spillback and lane blockage is able to significantly reduce the delay at congested intersections, as evidenced by the resulting total delay in MD 97 SB that is a near-oversaturated segment during the peak commuting period (i.e., 4,538 vehicles per hour).

Figure 0-25 reflects an interesting relationship between the MD97 SB delay and the receiving volume at off-ramp-H, where its total delay increased from 7439 vehicles at the low off-ramp volume to 9176.8 vehicle-minutes at the medium off-ramp volume, and then reduced to 6650.7 vehicle-minutes when the off-ramp volume reached the high level. This pattern exists regardless of using the proposed integrated model or TRANSYT-7F. It is due to the fact that both models are able to adjust the signal timing and cycle length to accommodate the increased volume from the increased off-ramp flows. For instance, the volume increase in MD97 SB from Intersection 2 to Intersection 4 demands an increase in their common cycle length and green split. The cycle lengths from the proposed model are 114 seconds, 142 seconds, and 164 seconds for low, medium, and high ramp volume, respectively. However, for drivers from all other intersection approaches, the increased volume on MD97 SB and the longer cycle length actually cause them to experience the higher total delay.

For MD 97 NB, the traffic volume stays at the constant level, but its total delay exhibited an increase because of the reduced green time split at signal 2 and the increased right-turn traffic from off-ramp H which generally result in an increased share of the total green duration.
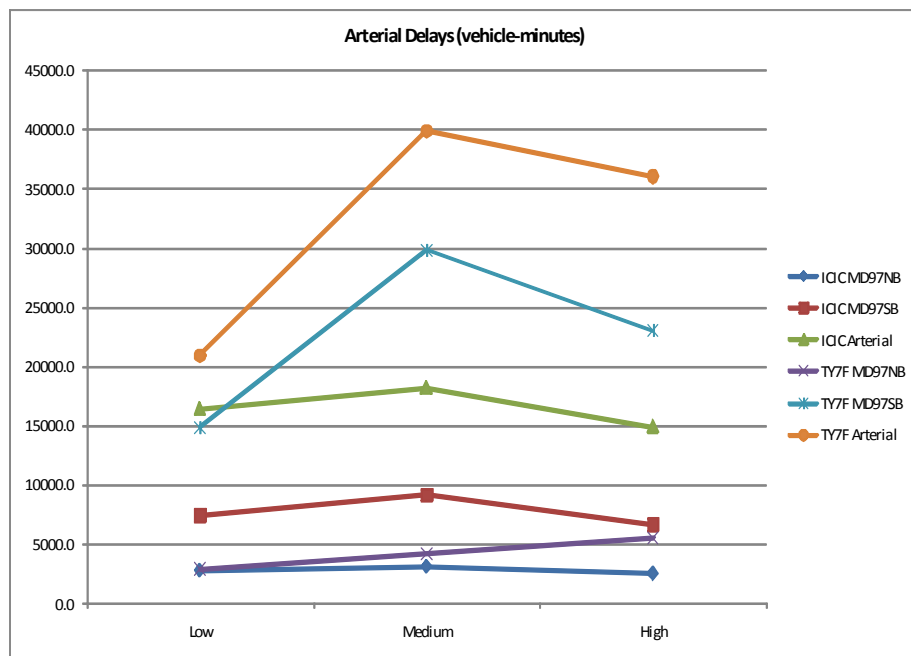

Figure 0-25 Comparison of arterial delay by segment

6.5   Conclusion

This chapter presents the evaluation results of the proposed integrated control models with both field data from the interchange between I-495 and George Avenue and simulation experiments. The results of extensive experimental analyses clearly indicate that the proposed models with its embedded formulations to capture the traffic interactions between congested flow movements can yield effective signal control plans to prevent the formation of lane blockage and queue spillback during near oversaturated traffic conditions. In fact, the proposed models significantly outperform the state-of-art signal model, TRANSYT-7F, with respect to all different MOEs at all different volume levels, regardless of including the freeway segment delay due to the off-ramp queue in the control objection function or not. With the proposed integrated interchange control model, one can decide the control objective based on the length of off-ramp queue spillback, and effectively uniform the congestion level for all arterial intersections within the interchange impact boundaries

CHAPTER 7: CONCLUSIONS AND RECOMMENDATIONS

7.1   Research findings

This study has presented an integrated control model to contend with the impact of off-ramp queue spillback on both the freeway and arterials within the interchange control boundaries. The proposed model consists of two levels that compute the optimal coordinated signal strategies for intersections and off-ramps. Whereas the first level primarily handles oversaturated flows and blockage between lanes at congested intersections, the second level deals with the freeway mainline delays caused by the excessive off-ramp queue spillback; these components work together to produce optimal system-wide signal and ramp control plans.

Since one or a few oversaturated intersection approaches on the congested arterial receiving freeway traffic may spill their queues either into neighboring lanes or back into their upstream intersections, the proposed integrated model with its embedded formulations can redistribute the congestion among all intersections within the control boundaries, minimizing — from the perspective of the entire system — both the average and longest delays. The proposed tool will allow responsible traffic agencies to design coordinated signal optimization plans for all intersections within an interchange's impact boundaries and to decide if freeway delay should be included in the optimization process. Thus, the tool makes it possible to prevent freeway bottlenecks caused by off-ramp queues from propagating through upstream segments, consequently paralyzing the entire freeway network.

In addition to developing control modules for oversaturated arterials and excessive off-ramp queues, the study also conducted some experimental analysis using field data from the interchange at I-495 and Georgia Avenue. The remainder of this section summarizes some key research findings from the extensive numerical results:

- The interchange's high off-ramp volume, in conjunction with the peak-hour arterial flow rates, will likely cause some intersection approaches to become oversaturated, consequently paralyzing traffic movements along the entire arterial.

- An oversaturated arterial adjacent to the interchange can cause different levels of congestion spillback at different intersection approaches; this oversaturation may also cause off-ramp queue lengths to extend beyond their auxiliary lanes, blocking the freeway's mainline lanes.

- State-of-art signal optimization programs, such as TRANSYT-7F, cannot yield effective signal control plans for oversaturated arterials that often experience lane blockage between neighboring lanes and queue spillback to their upstream segments.

- The proposed integrated model, with its embedded formulations — capable of capturing interactions between turning and through traffic flows, as well as congestion propagation between neighboring intersections — can effectively prevent the formation of local bottlenecks caused by queue spillback or lane blockage.

- This study shows that, by accounting for how off-ramp queues impact delays of both freeway and arterial traffic, the interchange system optimal control can yield the best use of a roadway's overall capacity and prevent the formation of freeway queues in the interchange area caused by the overflow of off-ramp traffic.

- The proposed integrated model can serve as an effective tool for responsible highway agencies to exercise the proper level of control based on the distribution of traffic volumes on freeway and arterials, as well as ramp queue lengths.

7.2   Recommendations for future studies

Building on the results of this study, we recommend that the following future tasks be conducted to effectively contend with the severe congestion patterns found around most urban freeway interchange areas:

- Enhance the computing efficiency of the current GA-based solution to ensure its applicability to a real-time control environment;

– Extend the integrated interchange model to include coordinated on-ramp metering control, as on-ramp queues may spill back into the local arterial when freeway volume approaches or exceeds its capacity;

– Generalize the formulations for the existing control model to handle multiple interchanges — which will include one freeway segment, several parallel or connected arterials, and multiple on- and off- ramps — since freeway congestion caused by excessively long off-ramp queues could spill back to an upstream interchange during peak hours;

– Develop a robust control algorithm capable of producing reasonably reliable results under the constraints of real-time data deficiencies, such as insufficient sensor information for input needs or measurement errors embedded in surveillance systems for computing the optimal control strategies;

– Integrate with advanced travel information systems to guide the distribution of traffic during congested peak periods, and

– Conduct field experiments to test the effectiveness of the proposed integrated control system under various real-world information constraints and uncertainty of driver responses to any implemented control strategies or guidance.

References

1. Abu-Lebdeh, G. and R. Benekohal (1997). "Development of traffic control and queue management procedures for oversaturated arterials." <u>Transportation Research Record: Journal of the Transportation Research Board</u> **1603**(-1): 119-127.

2. Abu-Lebdeh, G. and R. Benekohal (2000). "Genetic algorithms for traffic signal control and queue management of oversaturated two-way arterials." <u>Transportation Research Record: Journal of the Transportation Research Board</u> **1727**(-1): 61-67.

3. Abu-Lebdeh, G. and R. Benekohal (2003). "Design and evaluation of dynamic traffic management strategies for congested conditions." <u>Transportation Research Part A</u> **37**(2): 109-127.

4. Abu-Lebdeh, G., H. Chen, et al. (2007). "Modeling Traffic Output for Design of Dynamic Multi-Cycle Control in Congested Conditions." <u>Journal of Intelligent Transportation Systems</u> **11**(1): 25-40.

5. Ahn, S., R. Bertini, et al. (2007). "Evaluating Benefits of Systemwide Adaptive Ramp-Metering Strategy in Portland, Oregon." <u>Transportation Research Record: Journal of the Transportation Research Board</u> **2012**(-1): 47-56.

6. Allsop, R. (1971). "SIGSET: A computer program for calculating traffic capacity of signal-controlled road junctions." <u>Traffic Eng. Control</u> **12**: 58–60.

7. Allsop, R. (1976). "SIGCAP: A computer program for assessing the traffic capacity of signal-controlled road junctions." <u>Traffic Engineering & Control</u> **17**: 338-341.

8. Banks, J. (1993). "Effect of response limitations on traffic-responsive ramp metering." <u>Transportation Research Record</u> **1394**: 17-25.

9. Binning, J. C., G. Burtenshaw, et al. (2008). TRANSYT 13 User Guide, Transport Research Laboratory, UK.

10. Bogenberger, K. and A. May (1999). "Advanced coordinated traffic responsive ramp metering strategies." <u>California PATH Paper UCB-ITS-PWP-99-19</u>.

11. Boillot, F., J. M. Blosseville, et al. (1992). <u>Optimal signal control of urban traffic networks</u>. Road Traffic Monitoring, 1992 (IEE Conf. Pub. 355).

12. Cassidy, M. J., S. B. Anani, et al. (2002). "Study of freeway traffic near an off-ramp." <u>Transportation Research Part A: Policy and Practice</u> **36**(6): 563-572.

13. Ceylan, H. (2006). "Developing Combined Genetic Algorithm—Hill-Climbing Optimization Method for Area Traffic Control." <u>Journal of Transportation Engineering</u> **132**: 663.

14. Ceylan, H. and M. G. H. Bell (2004). "Traffic signal timing optimization based on genetic algorithm approach, including drivers' routing." <u>Transportation Research Part B</u> **38**(4): 329-342.

15. Ceylan, H., S. Haldenbilen, et al. (2010). "Development of delay models with quasi-Newton method resulting from TRANSYT traffic model." <u>Journal of Scientific & Industrial Research</u> **69**(2): 87-93.

16. Chang, E., S. Cohen, et al. (1988). "MAXBAND-86: program for optimizing left turn phase sequence in multiarterial closed networks." <u>Transportation Research Record</u> **1181**: 61-67.

17. Chang, G.-L., W. Jifeng, et al. (1994). "Integrated real-time ramp metering modeling for non-recurrent congestion: framework and preliminary results." <u>Transportation Research Record</u> **1446**: 56-65.

18. Chang, G., P. Ho, et al. (1993). "A dynamic system-optimum control model for commuting traffic corridors." <u>Transportation Research Part C: Emerging Technologies</u> **1**(1): 3-22.

19. Chang, T.-H. and J.-T. Lin (2000). "Optimal signal timing for an oversaturated intersection." <u>Transportation Research Part B</u> **34**(6): 471-491.

20. Chang, T. and G. Sun (2004). "Modeling and optimization of an oversaturated signalized network." <u>Transportation Research Part B</u> **38**(8): 687-707.

21. Chaudhary, N., A. Pinnoi, et al. (1991). "Proposed Enhancements to MAXBAND 86 Program." <u>Transportation Research Record</u> **1324**: 98-104.

22. Chen, C., J. B. Cruz, et al. (1974). "Entrance ramp control for travel rate maximization in expressways." <u>Transportation Research</u> **8**: 503-508.

23. Chen, C. I., J. B. Cruz, et al. (1974). "ENTRANCE RAMP CONTROL FOR TRAVEL RATE MAXIMIZATION IN EXPRESSWAYS." <u>Transportation Research</u> **8**(6): 503-508.

24. Chen, L., A. May, et al. (1990). "Freeway ramp control using fuzzy set theory for inexact reasoning." <u>Transportation research. Part A: general</u> **24**(1): 15-25.

25. Chen, O., A. Hotz, et al. (1997). <u>Development and evaluation of a dynamic ramp metering control model</u>. 8th IFAC(International Federation of Automatic Control)/IFIP/IFORS Symposium on Transportation Systems Chania, Greece.

26. Chlewicki, G. (2003). <u>New Interchange and Intersection Designs: The Synchronized Split-Phasing Intersection and the Diverging Diamond Interchange</u>. 2nd Urban Street Symposium: Uptown, Downtown, or Small Town: Designing Urban Streets That Work, Anaheim, CA.

27. Cremer, M. and S. Schoof (1989). "On control strategies for urban traffic corridors." <u>Proceedings of IFAC/IFIP/IFORS Symposium</u>: 213-219.

28. Daganzo, C. F. (1994). "The cell transmission model: a dynamic representation of highway traffic consistent with the hydrodynamic theory." <u>Transportation research. Part B: methodological</u> **28**(4): 269-287.

29. Daganzo, C. F. (1995). "The cell transmission model. II: Network traffic." <u>Transportation research. Part B: methodological</u> **29**(2): 79-93.

30. Dorothy, P., T. Maleck, et al. (1998). "Operational aspects of the Michigan urban diamond interchange." <u>Transportation Research Record: Journal of the Transportation Research Board</u> **1612**(-1): 55-66.

31. Engelbrecht, R. and K. Barnes (2003). "Advanced Traffic Signal Control for Diamond Interchanges." <u>Transportation Research Record: Journal of the Transportation Research Board</u> **1856**(-1): 231-238.

32. Fang, F. and L. Elefteriadou (2006). "Development of an Optimization Methodology for Adaptive Traffic Signal Control at Diamond Interchanges." <u>Journal of Transportation Engineering</u> **132**: 629.

33. Farzaneh, M. and H. Rakha (2006). "Procedures for Calibrating TRANSYT Platoon Dispersion Model." <u>Journal of Transportation Engineering</u> **132**(7): 548-554.

34. Gartner, N. (1983). "OPAC: A demand-responsive strategy for traffic signal control." Transportation Research Record **906**: 75-81.

35. Gartner, N., S. Assman, et al. (1991). "A multi-band approach to arterial traffic signal optimization." Transportation Research Part B: Methodological **25**(1): 55-74.

36. Gazis, D. C. and R. B. Potts (1963). The oversaturated intersection. 2th International Symposium on Traffic Theory, London, Organisation for Economic Co-operation and Development.

37. Gomes, G. and R. Horowitz (2006). "Optimal freeway ramp metering using the asymmetric cell transmission model." Transportation research. Part C, Emerging technologies **14**(4): 244-262.

38. Hadi, M. and C. Wallace (1995). "Treatment of Saturated Conditions Using TRANSYT-7F. ITE 65th Annual Meeting." Compendium of Technical Papers: 463–466.

39. Han, B. (1996). "Optimising traffic signal settings for periods of time-varying demand." Transportation Research Part A: Policy and Practice **30**(3): 207-230.

40. Henry, J., J. Farges, et al. (1984). The PRODYN real time traffic algorithm. Proceedings of the 4th IFAC, Transportation Systems, Pergamon.

41. Hou, Z., J.-X. Xu, et al. (2008). "An iterative learning approach for density control of freeway traffic flow via ramp metering." Transportation Research Part C: Emerging Technologies **16**(1): 71-97.

42. Hunt, P., R. Bretherton, et al. (1982). "SCOOT on-line traffic signal optimisation technique." Traffic Engineering and Control **23**: 190-2.

43. Improta, G. and G. E. Cantarella (1984). "Control system design for an individual signalized junction." Transportation Research Part B: Methodological **18**(2): 147-167.

44. Jacobson, L., K. Henry, et al. (1989). "Real-time metering algorithm for centralized control." Transportation Research Board **1232**: 17-26.

45. Jacobson, L., K. Henry, et al. (1989). "Real-time metering algorithm for centralized control." Transportation Research Board **1232**.

46. Jia, B., R. Jiang, et al. (2004). "Traffic behavior near an off ramp in the cellular automaton traffic model." Physical Review E **69**(5): 56105.

47. Kashani, H. and G. Saridis (1983). "Intelligent control for urban traffic systems." Automatica **19**(2): 191-197.

48. Kaya, A. (1972). Computer and optimization techniques for efficient utilization or urban freeway systems.

49. Kerner, B. (2005). "Control of spatiotemporal congested traffic patterns at highway bottlenecks." Physica A: Statistical Mechanics and its Applications **355**(2-4): 565-601.

50. Kim, J., J. Liu, et al. (1993). "The areawide real-time traffic control(ARTC) system: a new traffic control concept." IEEE Transactions on Vehicular Technology **42**(2): 212-224.

51. Kotsialos, A. and M. Papageorgiou (2004). "Efficiency and equity properties of freeway network-wide ramp metering with AMOC." Transportation Research Part C **12**(6): 401-420.

52. Kovvali, V., C. Messer, et al. (2002). "Program for optimizing diamond interchanges in oversaturated conditions." Transportation Research Record: Journal of the Transportation Research Board **1811**(-1): 166-176.

53. Lee, S., C. Messer, et al. (2006). "Actuated Signal Operations of Congested Diamond Interchanges." Journal of Transportation Engineering **132**: 790.

54. Levinson, D. and L. Zhang (2006). "Ramp meters on trial: Evidence from the Twin Cities metering holiday." TRANSPORTATION RESEARCH PART A-POLICY AND PRACTICE **40**(10): 810-828.

55. Li, M. and A. Gan (1999). "Signal timing optimization for oversaturated networks using TRANSYT-7F." Transportation Research Record: Journal of the Transportation Research Board **1683**: 118-126.

56. Li, Z., G.-L. Chang, et al. (2009). Integrated Off-Ramp Control Model for Freeway Traffic Management, Transportation Research Board.

57. Lighthill, M. and G. Whitham (1955). "On kinematic waves. II. A theory of traffic flow on long crowded roads." Proceedings of the Royal Society of London. Series A, Mathematical and Physical Sciences: 317-345.

58. Lin, W. and D. Ahanotu (1995). "Validating the basic cell transmission model on a single freeway link." PATH Technical Note **3**.

59. Lipp, L., L. Corcoran, et al. (1991). "Benefits of central computer control for Denver ramp-metering system." Transportation Research Record **1320**: 3-6.

60. Little, J., M. Kelson, et al. (1981). "MAXBAND: A program for setting signals on arteries and triangular networks." Transportation Research Record **795**: 40-46.

61. Little, J. D. C. (1966). "The Synchronization of Traffic Signals by Mixed-Integer Linear Programming." OPERATIONS RESEARCH **14**(4): 568-594.

62. Lo, H. K. (1999). "A novel traffic signal control formulation." Transportation Research Part A **33**(6): 433-448.

63. Lo, H. K., E. Chang, et al. (2001). "Dynamic network traffic control." Transportation Research Part A **35**(8): 721-744.

64. Lo, H. K. and A. H. F. Chow (2004). "Control Strategies for Oversaturated Traffic." Journal of Transportation Engineering **130**(4): 466.

65. Lovell, D. and C. Daganzo (2000). "Access control on networks with unique origin–destination paths." Transportation Research Part B **34**(3): 185-202.

66. Lovell, D. J. (1997). Traffic control on metered networks without route choice, University of California, Berkeley.

67. Masher, D., D. Ross, et al. (1975). "Guidelines for design and operation of ramp control systems." NCHRP Project 3-22 Final Report.

68. McCoy, P., E. Balderson, et al. (1983). "Calibration of Transyt Platoon Dispersion Model for Passenger Cars under Low-Friction Traffic Flow Conditions (Abridgment)." transportation Research Record **905**: 48-52.

69. Meldrum, D. and C. Taylor (1995). "Freeway traffic data prediction using artificial neural networks and development of a fuzzy logic ramp metering algorithm." Report No. WA-RD **365**.

70. Messer, C. and D. Berry (1975). "Effects of design alternatives on quality of service at signalized diamond interchanges." Transportation Research Record **538**: 20-31.

71. Messer, C., D. Fambro, et al. (1977). "Optimization of pretimed signalized diamond interchanges." Transportation Research Record **664**: 78-84.

72. Morgan, J. and J. Little (1964). "Synchronizing traffic signals for maximal bandwidth." OPERATIONS RESEARCH **12**(6): 896-912.

73. Munjal, P. (1971). An Analysis of Diamond Interchange Signalization, Highway Research Board.

74. Nihan, N. and D. Berg (1991). "Predictive Algorithm Improvements for a Real-Time Ramp Control System." Final Report GC8286 (16), WA-RD **213**.

75. Paesani, G., J. Kerr, et al. (1997). System wide adaptive ramp metering in southern California. ITS America 7th Annual Meeting.

76. Papageorgiou, M. (1980). "A new approach to time-of-day control based on a dynamic freeway traffic model." Transportation Research Part B: Methodological **14**(4): 349-360.

77. Papageorgiou, M. (1983). "A hierarchical control system for freeway traffic." Transportation Research Part B: Methodological **17**(3): 251-261.

78. Papageorgiou, M. (1990). "Modelling and real-time control of traffic flow on the southern park of Boulevard Peripherique in Paris: Part II: Coordinated on-ramp metering." TRANSP. RES. **24A**(5): 361-370.

79. Papageorgiou, M. (1995). "An Integrated Control Approach for Traffic Corridors." Transpn. Research. Part C, Emerging Technologies. **3**(1): 19-30.

80. Papageorgiou, M., J. M. Blosseville, et al. (1990). "Modelling and real-time control of traffic flow on the southern part of Boulevard Peripherique in Paris: Part I: Modelling." TRANSP. RES. **24A**(5): 345-359.

81. Papageorgiou, M., C. Diakaki, et al. (2003). "Review of Road Traffic Control Strategies." Proceedings of the IEEE **91**(12): 2043-2067.

82. Papageorgiou, M., H. Hadj-Salem, et al. (1991). "ALINE A: a local feedback control law for on-ramp metering."

83. Papageorgiou, M. and A. Kotsialos (2002). "Freeway ramp metering: An overview." IEEE Transactions on Intelligent Transportation Systems **3**(4): 271-281.

84. Park, B., C. Messer, et al. (2000). "Enhanced genetic algorithm for signal-timing optimization of oversaturated intersections." Transportation Research Record: Journal of the Transportation Research Board **1727**(-1): 32-41.

85. Park, B., C. J. Messer, et al. (1999). "Traffic Signal Optimization Program for Oversaturated Conditions: Genetic Algorithm Approach." Transportation Research Record **1683**: 133-42.

86. Payne, H., D. Brown, et al. (1985). Demand-responsive strategies for interconnected freeway ramp control systems. Volume 1: metering strategies, FHWA/RD-85/109, VERSAC Incorporated, San Diego, California.

87. Pooran, F. and R. Sumner (1996). Coordinated operation of ramp metering and adjacent traffic signal control systems, Report FHWA-RD-95-130. Federal Highway Administration, Washington DC, 1996.

88. Radwan, A. and R. Hatton (1990). "Evaluation Tools of Urban Interchange Design and Operation."

89. Reiss, R. A. (1981). "Algorithm development for corridor traffic control." Traffic, Transportation, and Urban Planning **2**.

90. Richards, P. (1956). "Shock waves on the highway." OPERATIONS RESEARCH: 42-51.

91. Robertson, D. (1969). "TANSYT: method for area traffic control." Traffic Engineering and Control **11**(6): 278-281.

92. Rudolph, G. (1994). "Convergence analysis of canonical genetic algorithms." IEEE transactions on neural networks **5**(1): 96-101.

93. Sasaki, T. and T. Akiyama (1986). Development of fuzzy traffic control system on urban expressway. Control in Transportation Systems, Vienna, Austria, Pergamon Press, Engl & New.

94. Schwartz, S. and H. Tan (1977). Integrated control of freeway entrance ramps by threshold regulation.

95. Seddon, P. (1972). "Another look at platoon dispersion: 3. The recurrence relationship." Traffic Engineering+ Control **13**: 442–444.

96. Sen, S. and K. Head (1997). "Controlled optimization of phases at an intersection." TRANSPORTATION SCIENCE **31**(1): 5-17.

97. Sims, A. and K. Dobinson (1980). "The Sydney coordinated adaptive traffic (SCAT) system philosophy and benefits." <u>IEEE Transactions on Vehicular Technology</u> **29**(2): 130-137.

98. Stamatiadis, C. and N. Gartner (1996). "MULTIBAND-96: a program for variable-bandwidth progression optimization of multiarterial traffic networks." <u>Transportation Research Record: Journal of the Transportation Research Board</u> **1554**: 9-17.

99. Stephanedes, Y. (1994). <u>Implementation of on-line zone control strategies for optimal ramp metering in the minneapolis ring road</u>, Institution of Electrical Engineers.

100. Stevanovic, A., P. Martin, et al. (2007). "VisSim-Based Genetic Algorithm Optimization of Signal Timings." <u>Transportation Research Record: Journal of the Transportation Research Board</u> **2035**(-1): 59-68.

101. Stringer, S. M. (2006) "Thinking outside the box: an analysis of Manhattan gridlock and spillback enforcement."

102. Tabac, D. (1972). <u>A linear programming model of highway traffic control</u>.

103. Taylor, C., D. Meldrum, et al. (1998). "Fuzzy ramp metering: design overview and simulation results." <u>Transportation Research Record: Journal of the Transportation Research Board</u> **1634**(-1): 10-18.

104. TIAN, Z. (2007). "Modeling and Implementation of an Integrated Ramp Metering-Diamond Interchange Control System." <u>Journal of Transportation Systems Engineering and Information Technology</u> **7**(1): 61-69.

105. Tian, Z., K. Balke, et al. (2002). "Integrated control strategies for surface street and freeway systems." <u>Transportation Research Record: Journal of the Transportation Research Board</u> **1811**(-1): 92-99.

106. Tian, Z., C. Messer, et al. (2004). "Modeling Impact of Ramp Metering Queues on Diamond Interchange Operations." <u>Transportation Research Record: Journal of the Transportation Research Board</u> **1867**(-1): 172-182.

107. Van Aerde, M. and S. Yagar (1988). "Dynamic integrated freeway/traffic signal networks: Problems and proposed solutions." <u>Transportation research. Part A: general</u> **22**(6): 435-443.

108. van den Berg, M., B. De Schutter, et al. (2004). Model predictive control for mixed urban and freeway networks. <u>Proceedings of the 83rd Annual Meeting of the Transportation Research Board</u>. Washington, DC. **19:** Paper 04-3327.

109. van den Berg, M., A. Hegyi, et al. (2003). <u>A macroscopic traffic flow model for integrated control of freeway and urban traffic networks</u>. Decision and Control, 2003. Proceedings. 42nd IEEE Conference on.

110. Venglar, S., P. Koonce, et al. (1998). "PASSER III-98 Application and User's Guide." <u>Texas Transportation Institute, Texas A&M Univ., College Station, Tex</u>.

111. Wang, C. F. (1972). "On a ramp-flow assignment problem." <u>TRANSPORTATION SCIENCE</u> **6**(2): 114-130.

112. Wang, J. and A. May (1973). <u>Computer model for optimal freeway on-ramp control</u>, Highway Research Board.

113. Wattleworth, J. (1963). "Peak-period control of a freeway system–some theoretical considerations." <u>Chicago area expressway surveillance project</u>.

114. Webster, F. (1958). <u>Traffic signal settings</u>, HMSO.

115. Webster, F. V. and B. M. Cobbe (1967). <u>Traffic Signals</u>, HMSO.

116. Wei, C.-H. and K.-Y. Wu (1996). "Applying an artificial neural network model to freeway ramp metering control." <u>Transportation Planning Journal</u> **25**(3): 335-356.

117. Wong, C. K., S. C. Wong, et al. (2007). "Reserve Capacity of a Signal-controlled Network Considering the Effect of Physical Queuing." <u>Transportation and Traffic Theory 2007: Papers Selected for Presentation at ISTTT17, a Peer Reviewed Series Since 1959</u>: 533.

118. Wong, S. C. and H. Yang (1997). "Reserve capacity of a signal-controlled road network." <u>Transportation Research Part B</u> **31**(5): 397-402.

119. Wu, J. and G. Chang (1999). "An integrated optimal control and algorithm for commuting corridors." <u>International Transactions in Operational Research</u> **6**(1): 39-55.

120. Xin, W., P. Michalopoulos, et al. (2004). "Minnesota's New Ramp Control Strategy: Design Overview and Preliminary Assessment." <u>Transportation</u>

Research Record: Journal of the Transportation Research Board **1867**(-1): 69-79.

121. Yoshino, T., T. Sasaki, et al. (1995). "The Traffic-Control System on the Hanshin Expressway." Interfaces **25**(1): 94-108.

122. Yuan, L. and J. Kreer "Adjustment of freeway ramp metering rates to balance entrance ramp queues."

123. Yuan, L. S. and J. B. Kreer (1971). "Adjustment Of Freeway Ramp Metering Rates To Balance Entrance Ramp Queues." Transportation Research **5**(2): 127-&.

124. Yun, I. and B. B. Park (2006). Application of stochastic optimization method for an urban corridor. Winter Simulation Conference, Monterey, California.

125. Zhang, H., J. Ma, et al. (2009). "Local Synchronization Control Scheme for Congested Interchange Areas in Freeway Corridor." Transportation Research Record: Journal of the Transportation Research Board **2128**(-1): 173-183.

126. Zhang, H. and S. Ritchie (1997). "Freeway ramp metering using artificial neural networks." Transportation Research Part C **5**(5): 273-286.

127. Zhang, M., T. Kim, et al. (2001). "Evaluation of on-ramp control algorithms." UC Berkeley: California Partners for Advanced Transit and Highways (PATH). Retrieved from: http://www. escholarship. org/uc/item/83n4g2rq.

128. Zhou, G., A. Gan, et al. (2007). "Optimization of Adaptive Transit Signal Priority Using Parallel Genetic Algorithm." Tsinghua Science & Technology **12**(2): 131-140.